BINDING PROPERTIES OF THE ADAPTOR PROTEINS TOLLIP AND TOM1

Mary Katherine Brannon

Thesis submitted to the faculty of the Virginia Polytechnic Institute and State University in partial fulfillment of the requirements for the degree of

Master of Science
In
Biological Sciences

Daniel G. S. Capelluto, Chair

David R. Bevan
Deborah F. Kelly
Jill C. Sible

April 16th, 2015
Blacksburg, VA

Keywords: Tollip, Tom1, endosomal trafficking, phosphatidylinositol-3-phosphate, cellular immunofluorescence, analytical ultracentrifugation, surface plasmon resonance, nuclear magnetic resonance

BINDING PROPERTIES OF THE ADAPTOR PROTEINS TOLLIP AND TOM1

Mary Katherine Brannon

ABSTRACT

Adaptor proteins, like Tollip and Tom1, facilitate cellular cargo sorting through their ubiquitin-binding domains. Tollip and Tom1 bind to each other through their TBD and GAT domains, respectively, whereas Tollip interacts with phosphatidylinositol-3-phosphate (PtdIns(3)P)-containing endosomal membranes. Tom1 and Tollip interaction and association with endosomes is proposed to be involved in the lysosomal degradation of polyubiquitinated cargo. Through cellular, biochemical, and biophysical techniques, we have further characterized the association of Tom1 with Tollip. Mutations in the binding interface of the Tom1 GAT and Tollip TBD complex leads to a subcellular mis-localization of both proteins, indicating that Tom1 may serve to direct Tollip to specific cellular pathways. It was determined that Tom1 inhibits the binding of Tollip to PtdIns(3)P and inhibition was reversed when mutations in the binding interface of the Tom1 GAT and Tollip TBD were present. Furthermore, it was established that, upon the binding of Tollip TBD to Tom1 GAT, ubiquitin is inhibited from binding to Tom1 GAT. It was also demonstrated that Tom1 GAT, but not Tollip TBD, can weakly bind to PtdIns(3)P. Consequently, we propose that association of Tom1 may serve to direct Tollip for involvement in specific cell signaling pathways. Gaining insight into the function of Tom1 and Tollip may lead to their use as therapeutic targets for increasing the efficiency of cargo trafficking and also for patients recovering from various cardiac injuries.

Dedication

I dedicate this thesis to my fiancé and my parents for supporting my dreams. Their love and support helped make this possible.

Acknowledgements

I would like to thank my advisor Dr. Daniel Capelluto and my committee members Drs. David Bevan, Deb Kelly, and Jill Sible for their guidance during my time here at Virginia Tech.

I would like to thank Dr. Shuyan Xiao for the work she did prior to me joining the project and I would also like to thank Xiaolin Zhao and Kristen Fread for all their help and support with this study, and for providing good conversation.

Table of Contents

List of Tables:

List of Figures:

Abbreviations:

APC	antigen-presenting cell
AUC	analytical ultracentrifugation
ARF	ADP ribosylation factor
BS^3	bis-sulfosuccinimidyl suberate
C1	protein kinase C conserved region 1
C2	protein kinase C conserved region 2
CUE	coupling of ubiquitin to ER degradation
DOPC	1,2-dioleoyl-sn-glycero-3-phosphate
EEA1	early endosomal antigen 1
Endofin	endosome-associated FYVE-domain protein
ER	endoplasmic reticulum
ESCRT	endosomal sorting complex required for transport
FYVE	Fab1, YOTB, Vacc1, EEA1
GAT	GGA and Tom1
GGA	Golgi-localizing, γ -adaptin ear domain homology, ADP ribosylation factor-binding
GST	glutathione S-transferase
HRP	horseradish peroxidase
Hrs	hepatocyte growth factor-regulated tyrosine kinase substrate
HSQC	heteronuclear single quantum coherence
IL-1R	interleukin-1 receptor
ILV	intraluminal vesicle

IRAK	interleukin receptor-associated kinase
K_D	dissociation constant
LIC	ligation-independent cloning
LPOA	lipid-protein overlay assay
LPS	lipopolysaccharide
MVB	multivesicular body
NF- κ B	nuclear factor kappa light chain-enhancer of activated B cells
NOE	nuclear Overhauser effect
PAMP	pathogen-associated molecular pattern
PtdIns(3)P	phosphatidylinositol-3-phosphate
PtdIns(5)P	phosphatidylinositol-5-phosphate
PtdIns(3, 4, 5) P_3	phosphatidylinositol-3, 4, 5-trisphosphate
PtdSer	phosphatidylserine
SPR	surface plasmon resonance
STAM	signal transducing adaptor molecule
TBD	Tom1-binding domain
TCTP	translationally-controlled tumor protein
TGN	*trans*-Golgi network
TIR	toll interleukin-1 receptor
TLR	Toll-like receptor
TNF α	tumor necrosis factor α
Tollip	Toll-interacting protein
Tom1	target of myb protein 1

UBA	ubiquitin-associated
UBD	ubiquitin-binding domain
UIM	ubiquitin-interacting motif
VHS	Vps27, Hrs, STAM

Chapter 1: Introduction

1.1 Literature review

1.1.1 Overview of plasma membrane and endosomal protein trafficking

The internalization of extracellular material such as fluid, macromolecules, particles, plasma membrane components, etc. is a necessary process to the life of prokaryotic and eukaryotic cells. This internalization process is called endocytosis and it begins with invagination of the plasma membrane and results in the formation of vesicles (or vacuoles), whose content can be degraded in the lysosomes, recycled back to the plasma membrane, or sorted for delivery to other organelles [9]. A cytosolic protein called clathrin is necessary for the formation of the transport vesicle. Clathrin associates with the cytosolic side of the plasma membrane and forms a basket-like structure that deforms the membrane [10]. In addition, clathrin functions to concentrate certain proteins within the endosome, through associations with an adaptor protein called adaptin and cargo receptors [10]. Upon separation from the plasma membrane, the clathrin coat dissociates from the vesicle, which will fuse to the early endosomal membranes (Fig. 1) [9]. The early endosome is a highly dynamic structure, as it serves mainly as a sorting station. The early endosome constantly receives vesicles from the plasma membrane and also departs vesicles to the plasma membrane for cargo recycling. Upon vesicle fusion with the

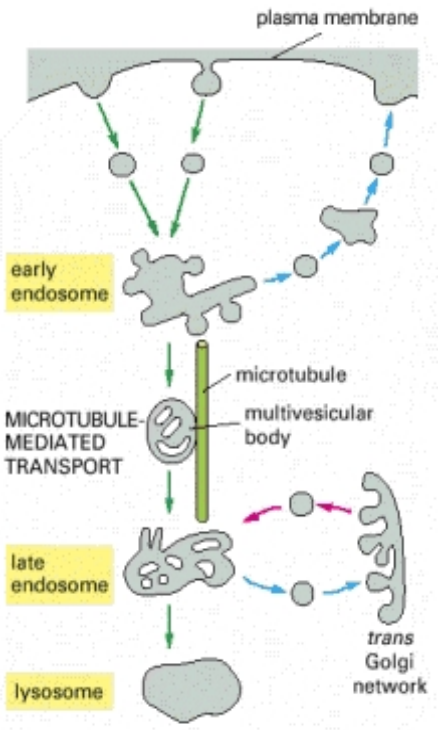

Figure 1: Maturation of endosome and transportation of material from the plasma membrane to lysosomes and the *trans*-Golgi network. Clathrin coats are utilized in the formation of endosomes and in the vesicles transporting material from the late endosome to the *trans*-Golgi network and viceversa. Taken from public domain source [1].

endosome, cargo is sorted to specific microdomains of the endosome, which dictate whether cargo gets recycled, degraded, or transported to the TGN. Intraluminal vesicles (ILVs) are formed within endosomes, which allows internalization of proteins found on the surface of the endosome (Fig. 1) [9, 11]. Endosomes containing ILVs become late endosomes as they mature and the pH begins decreasing. At this point, cargo within the late endosome has the opportunity to be transported to the *trans*-Golgi network (TGN) in clathrin coated vesicles (Fig. 1) [9]. The lysosome fuses with the late endosome, resulting in a further drop in pH, which then activates intraluminal enzymes that degrade the material remaining in late endosomes [9].

In addition to endocytosis, material may enter the cell through phagocytosis and autophagy. Phagocytosis functions for the cell to ingest foreign material, while autophagy functions for the cell to digest nonfunctional organelles (Fig. 2).

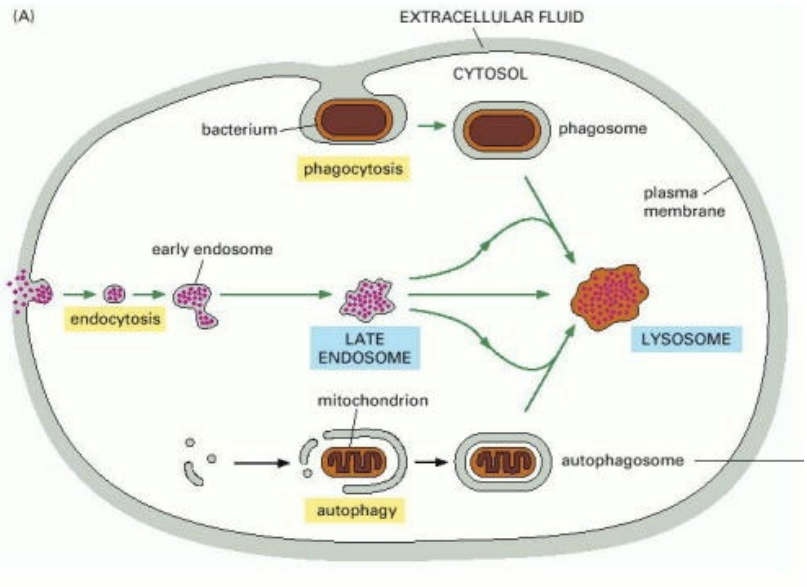

Figure 2: Material to be degraded in lysosomes reaches their destination in the lysosomes by one of three pathways: Material that originates in the extracellular environment can enter the cell through phagocytosis or endocytosis. In phagocytosis, all material ingested by the cell is degraded, while the rest of the material may be used for cellular processes. Material and organelles that originate from within the cell can be degraded in lysosomes using autophagy, in which old organelles and improperly folded proteins are transported from within the cell to lysosomes. Figure taken from public domain source [2].

1.1.2 Role of ubiquitin in the cell

Ubiquitin is an ubiquitous protein that can be covalently linked to other proteins to target them for degradation or to regulate protein structure, among other functions. Ubiquitin is covalently linked through its own C-terminal glycine (Gly76) to the lysine side chain amino groups that are located on a target protein. Proteins can be monoubiquitinated or polyubiquitinated, with each serving a specific function. Monoubiquitination typically regulates the protein structure, often leading to modification of the protein function, while polyubiquitination usually leads to degradation [12, 13]. The types of linkages in polyubiquitin chains may be varied, with each leading to degradation in a specific organelle or other function.

Ubiquitin is a small globular protein consisting of 76 amino acids and has an exposed and flexible C-terminus to allow for covalent bonding to other proteins. A three-step enzymatic process is necessary to ubiquitinate a protein. First, ubiquitin forms a bond with E1, an ubiquitin-activating enzyme that utilizes ATP for activation. After activation by E1, ubiquitin is transferred to E2, an ubiquitin-conjugating enzyme. During this step, thioester bonds are formed between ubiquitin and the cysteine residues of E1 and E2 [13]. An interaction between E2 and E3, a ubiquitin-ligating enzyme, finally transfers ubiquitin to a lysine on the target protein, forming an isopeptide bond (Fig. 3A) [13].

Many different forms of monoubiquitination and polyubiquitination occur within the cell, due to multiple lysine residues often being present in one protein and also in ubiquitin itself. Proteins that are polyubiquitinated can contain homotypic or heterotypic ubiquitin linkages. Ubiquitin contains seven lysine residues, which are found at the positions 6, 11, 27, 29, 33, 48, and 63. Therefore, polyubiquitin chains may link ubiquitin proteins at a combination of different lysine residues. Residues Lys6, Lys11, Lys27, Lys29, Lys33, and Lys48 are known to lead to

proteasome-mediated protein degradation, with Lys48 being the most preferred residue [3]. However, if a polyubiquitin chain utilizes the same lysine residue to form bonds between ubiquitin members (homotypic linkages) the resulting change in the cell or to the protein may be something different, such as DNA repair or lysosomal degradation rather than proteasome-mediated degradation (Fig. 3B) [3]. The remaining lysine in ubiquitin, Lys63, is not involved in polyubiquitin chains that lead to proteasome-mediated degradation. Lys63-linked polyubiquitin chains and monoubiquitination have been associated with endocytosis (Fig. 3B) [3, 14].

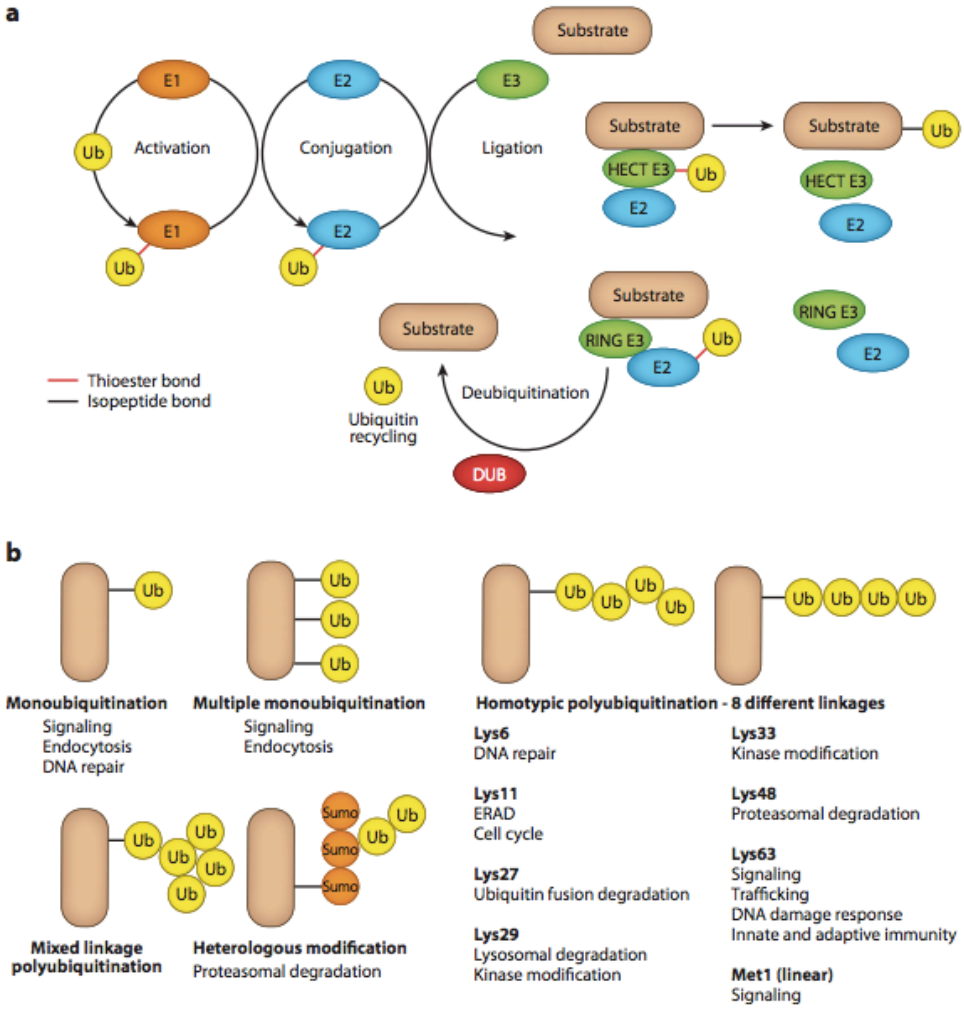

Figure 3: A. The activation and subsequent ligation of ubiquitin to various proteins or ubiquitin proteins utilizes 3 different enzymes, E1, E2, and E3. Covalent bonds are formed between the C-terminal glycine of ubiquitin and lysine residues that are found on the target protein or other molecules of ubiquitin. B. Different ways that ubiquitin is added on target proteins, and the subsequent result of ubiquitination of proteins in the cell. Taken from [3] with permission.

Ubiquitination plays a role in the degradation and regulation of transmembrane receptors, enzymes involved in cell signaling, and other proteins used by the cell. Without degradation and regulation of such receptors, downstream processes may experience excessive receptor activation that run amuck and cause imbalances in the cell, disrupting the normal metabolism and other processes necessary for the cell. Ubiquitination of proteins can target them for degradation. However, because transmembrane receptors may not be susceptible to degradation by proteasomes, they must be taken into the cell through endocytosis, and follow the endosomal pathway that leads to fusion with lysosomes [15]. Ubiquitin-binding domains (UBDs) are present in a variety of proteins, giving the proteins the ability to recognize ubiquitin modifications on targeted proteins by non-covalently binding to the ubiquitin moieties. Approximately twenty different families of proteins are known to contain UBDs, but most of these proteins interact with hydrophobic residues found in the region where Leu8, Ile44, and Val70 residues of ubiquitin (which is an otherwise polar protein) are located [3]. Proteins of importance to this study that contain UBDs are Tollip, which binds to ubiquitin through its C2 and CUE domains [6, 16], and Tom1, which binds to ubiquitin through its VHS and GAT domains [17-19].

1.1.3 The Role of Tom1 in endosomal trafficking

The gene encoding the target of myb protein 1 (Tom1) was originally found to be a target of a retroviral oncogene called *v-myb* [19]. However, more recently, Tom1 has been discovered to play a role in endosomal trafficking and sorting of proteins, due to its interactions with Tollip, ubiquitin, clathrin, and endosome-associated FYVE-domain protein (endofin) [7, 19-21]. Tom1 consists of 492 residues and contains an N-terminal VHS domain (residues 5-148) and a centrally located GAT domain (residues 212-312) (Fig. 4). The GAT domain is necessary for Tom1 to associate with Tollip, which is responsible for the recruitment of Tom1 to the

endosomal membrane surface [7, 19]. The GAT domain is known to interact with ubiquitin (monoubiquitin and polyubiquitin chains); therefore, it is likely that Tom1 is responsible for bringing ubiquitinated proteins to endosomes for their transport to the lysosomal pathway for their degradation [7, 17]. It has been reported that the VHS domain could also be required for Tom1 interaction with polyubiquitin chains, as it has been shown to directly bind ubiquitin [5, 18, 19]. Tom1 also binds to both endofin and clathrin simultaneously and it has been reported that endofin recruits clathrin via Tom1 [22].

Figure 4: Modular architecture of Tom1. Tom1 contains 2 functional domains: an N-terminal VHS domain and a central GAT domain. Taken from [4] with permission.

1.1.3.1 VHS structure and ubiquitin binding

The N-terminal VHS domain consists of about 140 residues, and it is present in many other proteins, including Vps27, Hrs, and STAM [18], hence the name VHS. These and other VHS-containing proteins may also have UBDs, FYVE (Fab1, YOTB, Vacc1, and EEA1) domains, which bind to endosomal phosphatidylinositol-3-phosphate (PtdIns(3)P) [5], and clathrin boxes [19].

The VHS domain assembles into a right-handed super helix, consisting of eight helices (Fig. 5), which contain residues that are conserved from yeast to humans [5, 19]. A common feature of most VHS domains is that they contain a recognition site for the acidic cluster-dileucine sequence, found in the cytoplasmic tail of the mannose 6-phosphate receptor [19]. Mannose 6-phosphate receptors function to concentrate lysosomal proteins in clathrin coated vesicles as they depart from the trans-Golgi network. However, the VHS domain of Tom1 does not contain the recognition site for mannose 6-phosphate receptors.

There is conflicting data about whether Tom1 VHS domain does actually bind ubiquitin.

It has been shown that the C-terminal portion of the VHS domain is necessary for binding to polyubiquitin chains, although it is not sufficient, as the residues between VHS and GAT domains, and the N-terminal portion of GAT are all required for Tom1 binding to ubiquitin [19]. Another report determined that almost all VHS domains bind to ubiquitin, including that Tom1 VHS, which binds to monoubiquitin with K_D value of 440 μM, as determined by surface plasmon resonance. This affinity is comparable to other VHS domain containing proteins also, such as Hrs [18]. These differences may very well be due to selective binding of monoubiquitin or polyubiquitin chains.

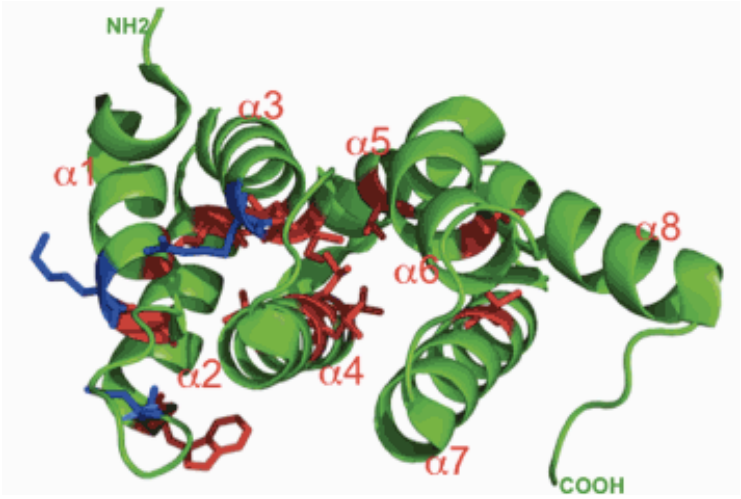

Figure 5: Structure of the VHS domain of Tom1. The VHS domain contains eight alpha helices (each labeled α1-α8). Residues shown in red are conserved hydrophobic residues, whereas residues shown in blue are conserved charged or polar residues. Taken from [5] with permission.

1.1.3.2 GAT structure and ubiquitin binding

GAT stands for GGA and Tom1, implying that the GAT domain is found in GGAs, which are Golgi-localizing, γ-adaptin ear domain homology, ADP ribosylation factor (ARF)-binding proteins, and in Tom1. GGAs are a well-characterized family of adaptor proteins that interact with clathrin and, therefore, regulate trafficking of cargo proteins as they leave the TGN and proceed to endosomes. The GAT domain of GGAs is known to recruit these proteins to the TGN and binds to GTPase ARF. GGAs also contain a proline-rich motif that simultaneously

recruits clathrin to the TGN membrane. However, the GAT domain of Tom1 does not bind ARF [17].

While the Tom1 GAT domain is smaller than the GAT domain found in GGAs, a three-helix bundle structure is predicted to be conserved between the two related proteins [19]. The GAT domain of Tom1 contains two binding sites for ubiquitin, the first spanning the C-terminal portion of helix α1 and the N-terminal portion of helix α2 (Fig. 6), whereas the second ubiquitin-binding site contains the N-terminal half of GAT helix α3 [4]. Despite both sites interacting with a hydrophobic patch of ubiquitin that includes Ile44, the interaction at Site 1 only weakly binds ubiquitin whereas the Site 2 strongly binds ubiquitin through residues Leu285 and Asp289. It is likely that the binding site of Tollip to the Tom1 GAT domain does not overlap with the ubiquitin binding Site 2, as mutating Leu285 and Asp289 did not affect binding of Tollip to the GAT domain [4]. Instead, it is possible that the binding of Tollip to the Tom1 GAT domain may displace the weakly bound ubiquitin at ubiquitin binding Site 1 [4].

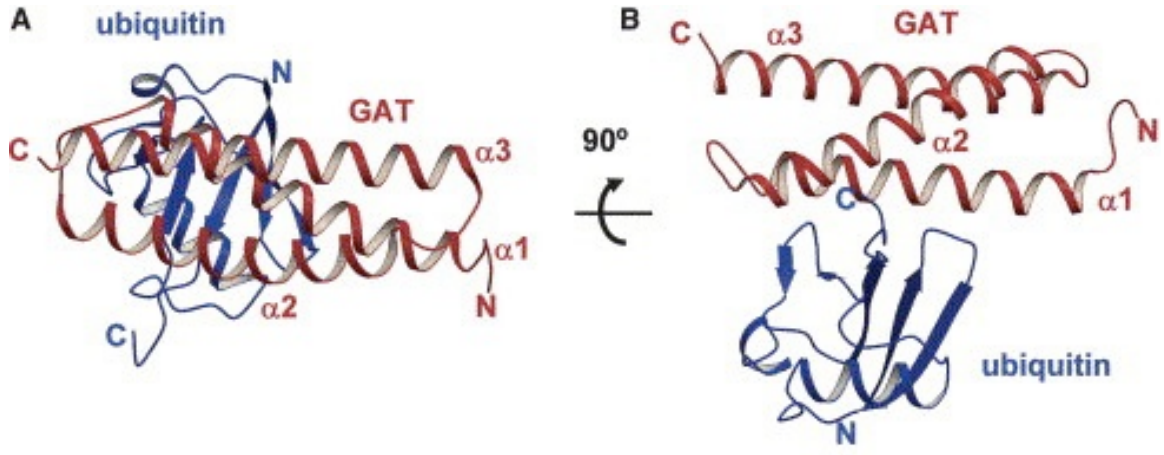

Figure 6: Two views of the crystal structure of the Tom1 GAT-ubiquitin Site 1 complex. At Site 1, ubiquitin Ile44 interacts with the C-terminus of helix α1 and the N-terminus of helix α2. Taken from [4] with permission.

1.1.3.3 Additional Tom1 ligands

Tom1 is also known to bind to Tollip through its GAT domain. The presence of the GAT

domain is not only necessary, but it is also sufficient for interaction with Tollip [19]. The GAT domain of Tom1 binds to an N-terminal domain of Tollip, called Tom1-binding domain (TBD) (Fig. 7) [7]. In addition to Tollip and ubiquitin, Tom1 also binds to clathrin heavy chain proteins found on endosomes [19, 21]. This binding occurs through a clathrin box in Tom1, which is commonly conserved between different organisms. The clathrin box is typically found in sequences following a pattern of polar residue, leucine, hydrophobic residue, polar residue, hydrophobic residue, and ending in a polar residue. The clathrin box of Tom1 is found at residues 321-326, and specifically has a sequence of Asp-Leu-Ile-Asp-Met-Gly [19]. Another ligand of Tom1 is endofin, a protein that is known to associate with PtdIns(3)P through its FYVE domain. The binding site of endofin is near the C-terminal region of Tom1. This association between Tom1 and endofin could be also responsible for the association of Tom1 with endosomal membrane compartments [20].

Through these simultaneous interactions between Tom1, Tollip, ubiquitinated proteins, and clathrin, a multi-protein complex is formed within the cell that potentially mediates an interaction between ubiquitinated proteins and endosomes. This complex could play a significant role in the lysosomal degradation of proteins.

A recent paper reported that Tom1, through its VHS and GAT domains, has the ability to bind to lipids, particularly PtdIns(5)P and PtdIns(3)P, through the use of protein-lipid overlay assays [23]. This is a novel concept, and is worth investigating as it is currently believed that Tom1 requires other adaptor proteins, like Tollip or Endofin, to associate with PtdIns(3)P enriched membranes. It seems likely that this PtdIns(3)P binding is relatively weak and that interaction occurs when levels of the phosphoinositide raise due to bacterial infection [24].

1.1.4 The role of Tollip in endosomal trafficking

The Toll-interacting protein (Tollip) is an adaptor protein that is most well known for interacting with the Toll family of proteins and interleukin-1, inhibiting innate immune responses. However, in addition to interacting with Toll-like receptors (TLRs) and interleukin-1 receptors (IL-1R), Tollip functions as an adaptor protein for endosomal protein trafficking. As mentioned previously, Tollip preferentially binds phosphoinositides, ubiquitin, and Tom1 [25, 26]. The interaction of Tollip and PtdIns(3)P is essentially responsible for the association of the Tom1, Tollip, and ubiquitinated protein complexes with endosomal membranes. Tollip protein consists of 274 residues and contains an N-terminal TBD, a central C2, and C-terminal CUE domains (Fig. 7) [6].

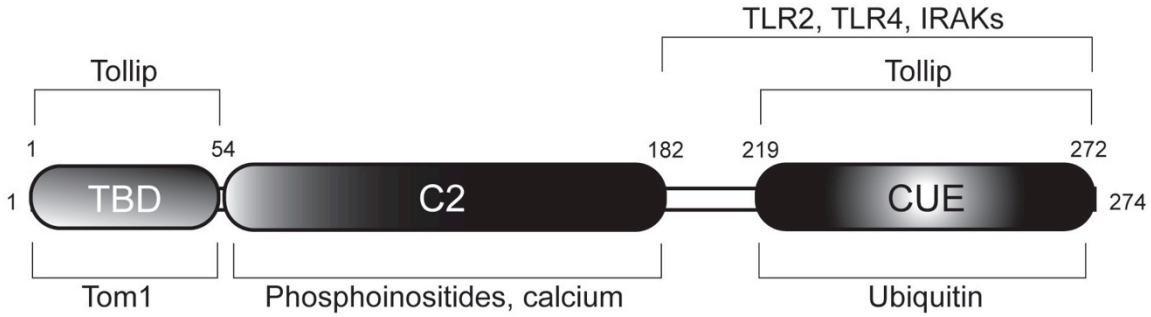

Figure 7: Tollip contains an N terminal TBD, which binds to the Tom1 GAT domain and may be involved in the oligomerization of Tollip. The central C2 domain preferentially binds phosphoinositides, responsible for the association of Tollip with endosomes, and calcium, whereas the C-terminus of the protein is involved in innate immunity and binding to TLRs and IRAKs. Taken from [6] with permission.

1.1.4.1 The Tollip TBD

The Tom1-binding-domain (TBD) is located at the N-terminus of Tollip. This domain interacts with the GAT domain of Tom1, allowing the endosomal recruitment of Tom1 [7]. Structural data obtained in the Capelluto laboratory indicates that Tollip TBD is an unfolded domain that partially folds when it contacts the Tom1 GAT domain (data not shown).

1.1.4.2 The Tollip C2 domain

Conserved 1 **(**C1) and conserved 2 (C2) domains are named for protein kinase C (PKC)

conserved regions 1 and 2, respectively [27]. Protein kinase C C2 domain is a lipid binding domain in which some C2 domains may bind calcium that is required for lipid binding [25, 27]. However, many C2-containing proteins have been reported that do not have the ability to bind calcium, yet can still bind to membranes. All C2 domains, regardless of their ability to bind calcium, consist of approximately 130 residues and share a fold of eight-stranded anti-parallel β-sandwich with loops connecting the β-strands, most of which are not conserved [27]. The C2 domain found in Tollip binds calcium, but this association is not necessary for phosphoinositide binding [25]. Specifically, the C2 domain of Tollip preferentially binds phosphoinositides, including PtdIns(3)P and phosphatidylinositol-3,4,5-trisphosphate (PtdIns(3,4,5)P_3) [25, 26]. Tollip C2 domain contains conserved basic residues that are necessary for binding PtdIns(3)P and PtdIns(3,4,5)P_3 [6]. The Tollip C2 domain has been found to bind to ubiquitin, and this binding decreases Tollip ability to bind PtdIns(3)P [28]. Through surface plasmon resonance (SPR), it was determined that the IC_{50} of ubiquitin inhibiting Tollip binding to PtdIns(3)P was 3.8 μM [28].

1.1.4.3 The Tollip CUE domain

The CUE domain also plays an essential role in endosomal trafficking pathways. CUE stands for coupling of ubiquitin to ER degradation and it is found at the C-terminus in Tollip. The CUE domain mediates dimerization, interacts with ubiquitin, TLRs, and IL1-Rs [6, 29, 30]. Because of its association with TLRs and IL-1Rs, the CUE domain is also essential for the function of Tollip in innate immunity.

CUE motifs are typically 42 to 43 amino acids long and all contain a conserved proline and di-leucine-like motifs [31]. CUE domains have been found to directly bind to ubiquitin [32]. CUE domains are structurally similar to ubiquitin interacting motifs (UIMs) and ubiquitin

associated (UBA) motifs as they seem to interact with ubiquitin in a similar manner [31]. All three (CUE, UIMs, UBA motifs) require Ile44 of ubiquitin for interaction and UBA and CUE domain both contain three α-helices, in addition to carrying a phenylalanine directly adjacent to the conserved proline [31]. CUE domains, in addition to IUM domains, are required for the ubiquitination of the protein within which the CUE or IUM domains are found. Therefore, the Tollip CUE domain is not only involved in binding ubiquitin modifications on proteins, but also it facilitates the direct ubiquitination of Tollip itself [28, 33].

The CUE domain is also necessary for interaction of Tollip with the IL-1 R. Upon activation by interleukin-1, IL-1 R is ubiquitinated and CUE domain binds the ubiquitinated IL-1 R. Degradation of the IL-1 R is then possible through entrance into MVBs, utilizing the association of Tollip with endosomes. In addition, it is proposed that ubiquitination of Tollip itself may cause the dissociation of IL-1R from the CUE domain [34].

1.1.4.4 The role of Tollip in innate immunity

The immune system consists of two different pathways for the elimination of a foreign pathogen from the host body. The first activated pathway is the innate immune system. Innate immunity is perhaps the most primitive of the two pathways, but it is also the most efficient as it eliminates pathogens immediately through the recognition of pathogen-associated molecular patterns (PAMPs). The second activated pathway by foreign pathogens is the humoral immune system, in which foreign antigens are presented by professional antigen-presenting cells (APCs), including macrophages, dendritic cells, and B cells. The APCs activate B cells to produce antibodies specific to the foreign antigen they are presenting. Antibodies specific to a pathogen can further target pathogens for attack by the humoral immune system. While the humoral immune system is more sophisticated and specific than the innate system, the latter acts quicker,

as the humoral system may take several weeks to months and multiple exposures to produce a sufficient titer of antibodies to target specific pathogens. Tollip plays a role in the innate immune system, as it is believed to negatively modulate this pathway upon activation by a foreign pathogen.

TLRs are expressed on the surface of many different types of cells found within the host body, as well as on the endoplasmic reticulum (ER), endosomes, lysosomes, and endolysosomes [6]. These receptors recognize PAMPs found on foreign pathogens and act first to alert the innate immune system of the presence of a pathogen. PAMPs are found within proteins or other molecules that originate only in foreign pathogens. This allows the host organism to distinguish between host and foreign molecules in order to activate the innate immune system. For example, gram-negative bacteria contain lipopolysaccharides (LPS) on their membranes that are associated only with bacteria and LPS is a PAMP recognized by TLRs, particularly TLR4 [35, 36]. Once activated by PAMPs, plasma membrane TLRs communicate with the cytosol through the association of adaptor proteins on the cytosolic side of the receptor. This signaling ultimately activates transcription factors, particularly NF-κB, which regulates the transcription of certain pro-inflammatory cytokines, such as IL-1 and TNFα [6, 37]. MyD88 is one of the adaptor proteins that interacts with Toll-interleukin-1 receptor (TIR) domains of all TLRs in addition to IL-1Rs [6]. The association of MyD88 with cytosolic TIR domains of TLRs allows recruitment of the interleukin-4 receptor-associated kinase (IRAK-4). IRAK-4 auto-phosphorylates itself once activated, and more adaptor proteins are subsequently recruited to lead to the activation of NF-κB [6].

The role of Tollip in the innate immune system occurs at two levels. Tollip first can directly associate with TLRs and IL-1R upon activation and can inhibit a signal from being

communicated to the inside of the cell. In addition, Tollip can bind to IRAK-1 preventing its auto-phosphorylation, which in turn, impairs binding of other adaptor proteins involved in the activation of NF-κB [6]. Through these interactions, Tollip can inhibit the activation of the innate immune system, which can have positive and negative results. For patients suffering from an over-active immune system and experiencing conditions of chronic inflammation, the inhibition of the innate immune system could reduce levels of inflammation.

1.1.5 Intracellular complexes involving Tom1 and Tollip

It is predicted that Tom1, Tollip, ubiquitinated cargo proteins, clathrin, and endofin form a complex that associates with endosomes; however, not much is known about the function of this complex. As indicated above, Tom1 and Tollip form an association with each other through their GAT and TBD domains, respectively. Through this association, ligands of one protein could be associated with ligands of the other, unless there is competition for the same site. Therefore, binding of ubiquitin/ubiquitinated proteins, clathrin, and endofin will be associated with endosomes because of the interaction of Tollip with PtdIns(3)P, a phospholipid that is exclusively enriched in endosomal membranes (Fig. 8) [7].

The ability of the complex to associate with ubiquitinated proteins can perhaps help direct ubiquitinated proteins to lysosomes for degradation. Upon association with endosomes, ubiquitinated proteins may be sorted and subsequently end up in luminal vesicles of MVBs, and then ultimately delivered to lysosomes [7]. It is also a possibility that monoubiquitinated proteins not destined for degradation may be bound to this complex of Tom1 and Tollip, sorted and delivered to destinations other than lysosomes.

Another possible function of the complex containing Tom1 and Tollip is that it may be responsible for the recruitment of clathrin to endosomes. As mentioned previously, one of the

ligands of Tom1 is clathrin, the adaptor protein involved in the formation of transport vesicles from the plasma membrane and TGN. Tollip does not directly recruit clathrin to endosomes, as only Tom1 contains the clathrin box, but Tollip association with Tom1 subsequently recruits clathrin [21]. This recruitment of clathrin by Tom1 and Tollip is likely essential for the formation of transport vesicles containing ubiquitinated cell surface receptors. The recruitment of clathrin by Tollip and Tom1 could also be responsible for the formation of transport vesicles used for the purpose of recycling cargo back to the cell surface from endosomes. Evidence for this was seen in immunofluorescence studies in which HeLa cells that expressed Tom1 alone were found to have endogenous clathrin that was mostly located throughout the cytosol, similar to where Tom1 was found in this case [21]. The expression in HeLa cells of Tollip by itself had no effect on the localization of clathrin. However, clathrin, Tom1 and Tollip were all found to be localized on endosomes in cells that simultaneously overexpressed Tollip and Tom1 [21].

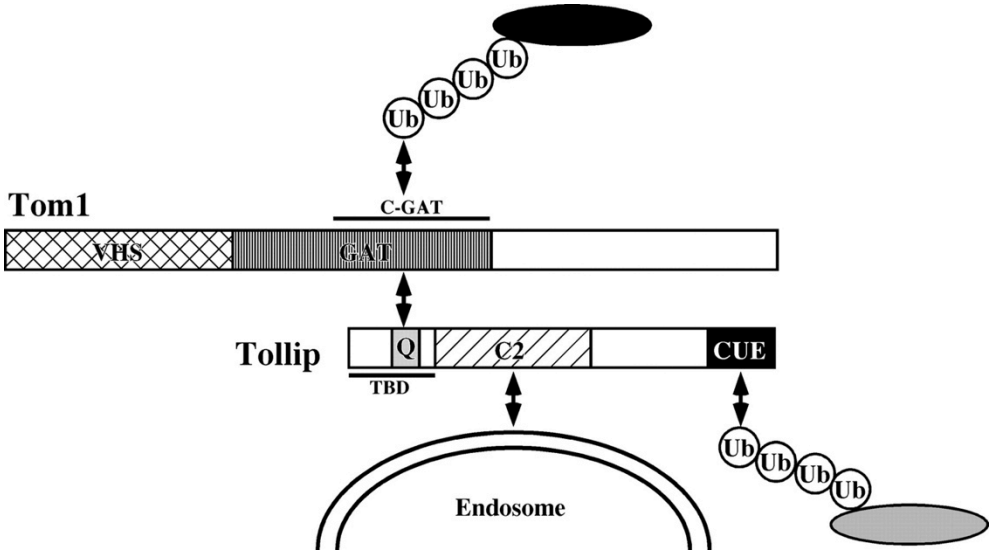

Figure 8: Tollip associates with PtdIns(3)P-enriched endosomal membranes through its C2 domain. Tollip then recruits ubiquitinated proteins to its CUE domain and Tom1 to its TBD domain. The recruitment of Tom1 to Tollip then indirectly recruits additional ubiquitinated proteins. Therefore, ubiquitinated proteins can be brought in close association to endosomes, which may lead to their degradation. Taken from [7] with permission.

1.1.6 The function of the ESCRT machinery in endosomal protein trafficking

In addition to Tom1 and Tollip, many other adaptor proteins are known to function in the recruitment of ubiquitinated protein cargo to endosomes. The best characterized is the endosomal sorting complex required for transport (ESCRT) machinery, which plays a role in the formation of MVBs. Specifically, the ESCRT machinery is responsible for the sorting and transportation of cargo proteins into these MVBs as well as for pinching off the vesicles found within MVBs [8]. The ESCRT machinery consists of protein complexes ESCRT 0, I, II, and III [38]. ESCRT 0, consists of the hepatocyte growth factor-regulated tyrosine kinase substrate (Hrs) and the signal transducing adapter molecule (STAM). Hrs is responsible for association of ESCRT-0 to endosomal membranes through its FYVE domain, which binds to PtdIns(3)P. Hrs and STAM each consists of a GAT and VHS domain. GAT domains intertwine with each other, forming the association between Hrs and STAM, whereas the VHS domain binds ubiquitin [39]. In addition, these subunits contain a clathrin-binding domain, which recruits clathrin to assist in the deformation of the membrane for vesicle formation. The complex formed between Tollip, Tom1, and their other ligands could be representative of the ESCRT 0 complex (also known as ESCRT 0-like complex). Tollip anchors to endosomal membranes through its C2 domain, which binds PtdIns(3)P. Tom1 is very similar to Hrs and STAM, in that it consists of VHS and GAT domains and has a clathrin-binding site. In addition, the Tom1 VHS domain is known to weakly bind monoubiquitin [18]. Other adaptor proteins are known to recruit polyubiquitinated proteins to endosomal membranes, including Tom1, Tollip, and Endofin. It is not clear whether the Tom1-Tollip complex simply overlaps in function with the ESCRT machinery or whether ESCRT machinery and the Tom1-Tollip complex interact with each other. Figure 10 [8] displays a diagram of the overlap/interaction of the multiple protein complexes, including Tom1 and Tollip, that could function as the “ESCRT 0” complex.

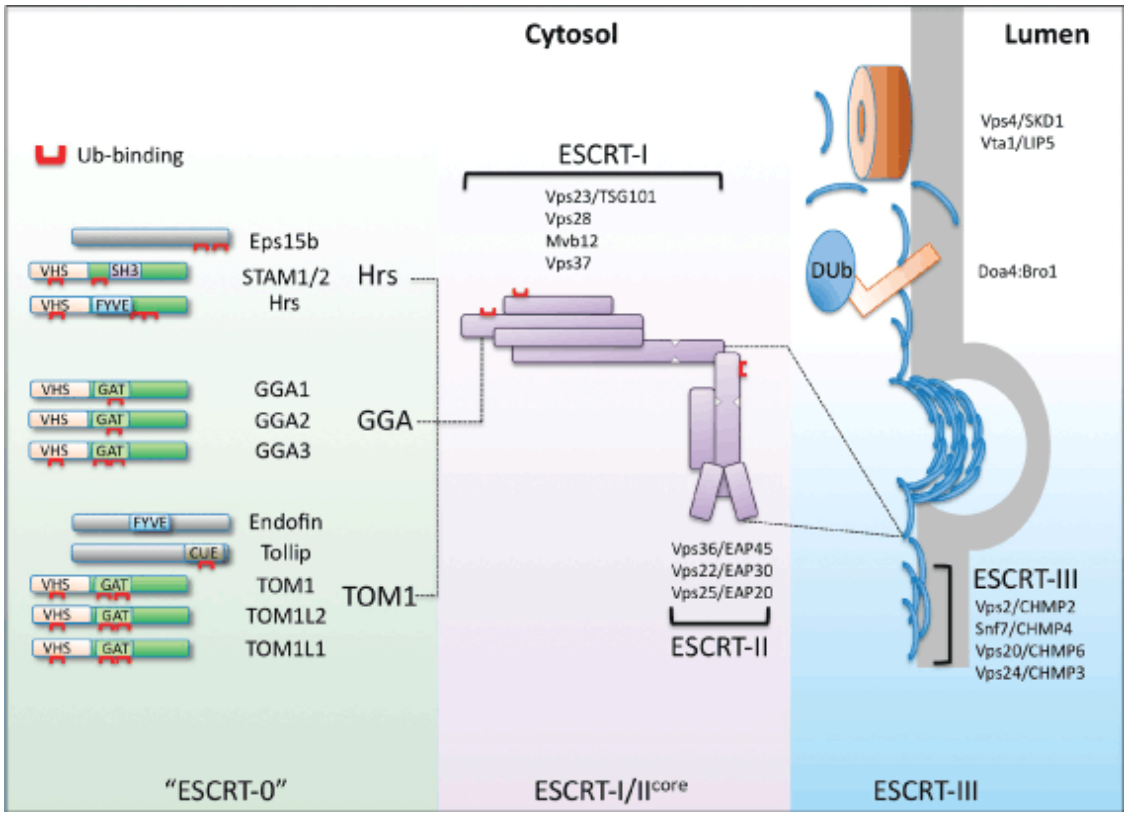

Figure 9: ESCRT machinery and the composition of "ESCRT 0", ESCRT I/II, and ESCRT III complexes. It is suggested that multiple complexes of proteins (Hrs, GGA, and Tom1) can serve as ESCRT 0 as they seem to have some overlapping functions. Taken from [8] with permission.

1.2 Hypothesis

The goal of this study was to functionally characterize the association between endosomal adaptor proteins Tom1 and Tollip. The study was designed based on the hypothesis that Tom1 and Tollip must work together for the recruitment and/or delivery of ubiquitinated cargo to endosomal membranes.

1.3 Objectives

The following specific objectives were set to carry out and test the hypotheses:

1.3.1 To disrupt the subcellular co-localization of Tollip and Tom1.

When over-expressed simultaneously, Tom1 has been shown to co-localize with Tollip on punctate structures *in vivo*. However, when over-expressed alone, Tom1 was diffusely localized to the cytosol of the cell. Cell-based immunofluorescence studies were conducted in

HeLa cells to determine whether a subcellular mis-localization of Tom1 occurs when the association between Tom1 and Tollip is disrupted.

1.3.2 To determine the effect of Tom1 on Tollip binding to PtdIns(3)P.

While it is known that Tom1 binds to Tollip, it is not known whether the binding of Tom1 to Tollip increases (or decreases) the affinity of Tollip for PtdIns(3)P. Lipid-protein overlay assays were used to characterize the affect of Tom1 on Tollip binding to PtdIns(3)P.

1.3.3 To determine whether Tollip TBD and Tom1 GAT bind PtdIns(3)P.

It has been recently reported that Tom1 GAT can bind to PtdIns(3)P and recent data (not shown) hinted that Tollip TBD may bind to PtdIns(3)P. Nuclear magnetic resonance (NMR) and SPR experiments were performed to determine whether Tollip TBD and Tom1 GAT bind to PtdIns(3)P.

1.3.4 To determine whether Tom1 GAT can simultaneously bind Tollip TBD and ubiquitin

Tom1 GAT is known to have two ubiquitin binding sites; however, it is not known if ubiquitin(s) remain bound to Tom1 GAT when Tollip TBD is also bound to GAT. Analytical ultracentrifugation experiments were performed to address this hypothesis.

1.4 Significance:

Adaptor protein-mediated membrane trafficking of proteins is critical in cellular functions of membrane excitability and cardiomyocyte physiology. Deficient membrane trafficking function contributes to a wide range of cardiovascular diseases, including Ab-lipoproteinemia, Brugada syndrome, familial hypercholesterolemia, long QT-2 syndrome, and myotubular myopathy, to name a few [40]. Specifically, Tollip modulation of TLR signaling is also relevant for heart function. Activation of the TLR signaling pathway plays a major role in the development and progression of atherosclerosis, septic cardiomyopathy, ischemia and

reperfusion injury, cardiac hypertrophy, and congestive heart failure [41-46]. Indeed, Tollip has been shown to act as a negative regulator during the development of cardiac hypertrophy by attenuating the function of IL-1 β [44]. Recently, Tollip has been demonstrated to serve as a negative regulator of pathological cardiac hypertrophy blocking the AKT signaling pathway [47]. Whereas there are not yet studies of Tom1 associated with cardiovascular diseases, there is no doubt that Tollip is a potential therapeutic protein for patients experiencing heart failure due to pressure overload-induced cardiac hypertrophy. Additionally, Tom1 and Tollip could be targeted to compensate for deficient cargo trafficking in patients suffering from diseases mentioned above.

Chapter 2: Materials and Methods

2.1 Materials

1,2-dioleoyl-sn-glycero-3-phosphocholine (DOPC); phosphatidylinositol-3-phosphate (PtdIns(3)P). All other materials purchased were of analytical grade.

2.2 Methods

2.2.1 Ligation-independent cloning (LIC)

The LIC vector pCS-3XFLAG-LIC was first digested with restriction enzyme BseRI (NEB) to linearize the vector at the LIC site, and later treated with T4 DNA Polymerase (Novagen) in the presence of dTTP, creating single stranded noncompatible overhangs. Tom1 PCR products contained the following sequences complementary to single strand overhangs of the treated LIC vector: The sequence 5'-GAC GAC GAC AAG ATG was added to the 5' –end of the sense DNA strand with ATG being the start codon used by Tom1, while the sequence 5'-GAG GAG AAG CCC GGT was added to the 5' end of the anti-sense strand. Tom1 PCR products were treated with T4 DNA Polymerase in the presence of dATP following purification of PCR product. Vector and insert were then incubated at a ratio of 1:2 for 5 min at 22°C, followed by addition of 25 mM EDTA, with another 5 min incubation at 22°C. The annealing reaction was used for the transformation of bacterial cells.

2.2.2 Site-directed mutagenesis and protein overexpression for cellular-based immunofluorescence assays.

Human Tom1 and Tollip cDNAs were cloned into pCS-3XFLAG-LIC and pEGFP-C1 plasmids, respectively. Tom1 and Tollip mutants were created by alanine scanning mutagenesis into Tom1 and Tollip constructs using the Quick Change method. All mutants and resulting sequence are shown in Table 1. HeLa (American Type Culture Collection) cells were maintained

in a 37 °C humidified incubator in the presence of 5% CO_2 in DMEM with 10% heat-inactivated fetal bovine serum (Sigma), 25,000 U/L penicillin, and 25 mg/L streptomycin. Cells were regularly split at approximately 70% confluency. Approximately 10^6 cells were grown on glass coverslips and Lipofectamine LTX (Invitrogen) was used to induce transient transfection at 2.2 µL Lipofectamine LTX to 1 µg DNA. Transfections were performed in OptiMEM I Reduced Serum Medium (Invitrogen). Cells were then allowed to overexpress Tom1 and Tollip proteins for approximately 12-16 h in the conditions described above for maintenance of cells.

Table 1: Sequence and name of each EGFP-Tollip and 3X-FLAG-Tom1 primers designed for site-directed mutagenesis.

Tom1 or Tollip mutant primer name	Primer sequence
EGFP-Tollip R9A/V12A	Forward: 5'- TCA GCA CTC AGG CCG GGC CGG CGT ACA TCG GTG -3' Reverse: 5'- CAC CGA TGT ACG CCG GCC CGG CCT GAG TGC TGA -3'
EGFP-Tollip D20A/R23A	Forward: 5'- GCT CCC GCA GGC CTT CCT CGC CAT CAC GCC CA -3' Reverse: 5'- TGG GCG TGA TGG CGA GGA AGG CCT GCG GGA GC -3'
EGFP-Tollip F21A	Forward: 5'- GCT CCC GCA GGA CGC CCT CCG CAT CAC G -3' Reverse: 5'- CGT GAT GCG GAG GGC GTC CTG CGG GAG C -3'
EGFP-Tollip F21A/L22A	Forward: 5'- GAG CTC CCG CAG GAC GCC GCC CGC ATC ACG CCC AC -3' Reverse: 5'- GTG GGC GTC ATG CGG GCG GCG TCC TGC GGG AGC TC -3'
3X-FLAG-Tom1 E223A/R267A	E223A primer pair: Forward: 5'- GAA GCT GCG CAG TGC GCT GGA GAT GGT GAG -3' Reverse: 5'- CTC ACC ATC TCC AGC GCA CTG CGC AGC TTC -3' R267A primer pair: Forward: 5'- GAG CCA TGC AGC AGG CGG TCC TGG AGC TG -3' Reverse: 5'- GAG CTC CAG GAC CGC CTG CTG CAT GGC TC -3'
3X-FLAG-Tom1 N230A	Forward: 5'- GAT GGT GAG TGG GGC CGT GAG GGT GAT G -3' Reverse: 5'- CAT CAC CCT CAC GGC CCC ACT CAC CAT C -3'

3X-FLAG-Tom1 L257A	Forward: 5- GCT GCT GCA GGA GGC CAA CCG CAC GTG C -3' Reverse: 5'- GCA CGT GCG GTT GGC CTC CTG CAG CAG C -3'

2.2.3 Immunofluorescence analysis.

Cells grown on glass coverslips were fixed and permeabilized in 3.7% formaldehyde 0.5% Triton X-100 in PBS for 7 min at room temperature and blocked for 30 min in 20% goat serum in PBS. Primary antibodies Sigma Mouse ANTI-FLAG M2 antibody (F3165) and BD ANTI-EEA1 antibody were incubated with cells at appropriate dilution in 0.1% Triton X-100, PBS at 4°C overnight followed by incubation with a secondary antibody, Cy 3-conjugated Goat anti-mouse antibody (Jackson ImmunoResearch) for 1 h at room temperature. Washes were performed after fixing/permeabilization and in between each antibody incubation using 0.1% Triton X-100 in PBS. Coverslips were mounted onto glass slides (Fisher) with elvanol mounting medium. Images were analyzed with fluorescence microscope Nikon Eclipse TE2000-E equipped with a Prairie sweptfield confocal system. A 100X Nikon Plan-Apo oil immersion objective with numerical aperture of 1.40 was used. Images were captured with a Cascade II camera (Photometrics) and NIS-Elements AR 4.2 software (Nikon).

2.2.4 Protein overexpression and purification from bacterial cells

Human Tom1 cDNA was cloned into pET28a plasmid, whereas human Tollip, Tollip TBD (residues 1-53), and Tom1 GAT (residues 215-309) cDNAs were cloned into pGEX6P-1. Proteins were overexpressed in *Escherichia coli* Rosetta (Tom1, Tom1 GAT) or Rosetta (DE3) (Tollip, Tollip TBD, Tom1 GAT) cells. Bacterial cells were grown overnight in a small volume of Luria-Bertani (LB) broth at 37ºC and then added to larger volumes of LB broth and allowed to grow until reaching an optical density of ~0.8. Cell cultures were then induced with 1 mM isopropyl β-D-thiogalactopyranoside at 25 ºC for 4 h. For NMR experiments, ^{15}N-labeled proteins

were produced in minimal media containing ^{15}N ammonium chloride. Cell cultures were then centrifuged to pellet cells. Three cycles of freeze and thaw (at -80°C and 4° C) were performed on the cell pellets. Cells expressing glutathione S-transferase (GST) fusion proteins were resuspended in 50 mM Tris-HCl (pH 8), 250 mM NaCl, 1 mM DTT, 0.1 mg/ml lysozyme, and 0.1 % Triton X-100 on ice, at a volume of 80 mL per 1 L of pelleted cell cultures. Cells expressing His-tag proteins were resuspended in 50 mM sodium phosphate (pH 8), 300 mM NaCl, 0.1 mg/ml lysozyme, 1 mM β-mercaptoethanol, and 0.1 % Triton X-100 on ice, at a volume of 80 mL per 1 L pelleted culture. Cell resuspensions were then sonicated on ice no more than 4 times in 30-second cycles. Crude extract was centrifuged at 10,000 rpm for 45 min at 4° C. and the resulting supernatant was incubated for 1 h (GST-tagged proteins) or 30 min (His-tagged proteins) at 4° C with glutathione beads (GE Healthcare) and nickel chelating resin, respectively. Glutathione beads (containing GST-Tollip, GST-Tollip TBD, or GST-Tom1 GAT) were then washed with 20 mM Tris-HCl (pH 8), 500 mM NaCl, and 1 mM DTT. GST Tollip was eluted from the glutathione beads with elution buffer (20 mM Tris-HCl (pH 8), 500 mM NaCl, 100 mM reduced gluthathione, and 1 mM DTT). GST-Tollip TBD proteins were cleaved by incubation with HRV 3C protease (Pierce) at 25 U/mL beads for 3 h at room temperature, while GST-Tom1 GAT was cleaved by incubation with HRV 3C protease (Pierce) at 40 U/mL beads for 8 h at room temperature. GST-Tollip was then concentrated by the use of 10-kDa molecular weight cut off centrifugal filter units (Millipore) while Tollip TBD and Tom1 GAT were concentrated by similar centrifugal units of 3-kDa molecular weight cut off. Nickel chelating beads (His-Tom1) were washed with His-tag buffer containing 20 mM imidazole. The addition of 200 mM imidazole to the His-tag buffer was used to elute the His-tagged protein. His-Tom1 was then concentrated by the use of 10 kDa molecular weight cut off centrifugal filter units. Proteins were then purified further through the use of gel

filtration on Superdex columns previously equilibrated with 20 mM Tris-HCl (pH 8), 500 mM NaCl, 1 mM DTT, and 1 mM NaN_3 buffer. The appropriate fractions containing the protein of interest were then pooled and concentrated. Buffer was exchanged using centrifugal filter units, if necessary, and then protein concentrations were measured using bicinchoninic acid or Bradford protein assay reagent [48].

2.2.5 Lipid-protein overlay assay

Hybond-C Extra (GE Healthcare) nitrocellulose membranes were spotted with 1 µL of the appropriate concentration of PtdIns(3)P in a solution of chloroform:methanol:water (65:35:8). Membranes were allowed to dry for 1 h at room temperature and were then blocked with 3% (w/v) fatty-acid-free BSA (Sigma) in 20 mM Tris-HCl (pH 8.0), 150 mM NaCl, and 0.1 % Tween-20 for 1 h at room temperature. Membranes were then incubated overnight at 4°C with GST-fusion proteins or GST-fusion proteins that were preincubated with two- to four-fold excess molar ratios of either Tom1, Tom1 GAT, or ubiquitin. Three washes were performed with the same buffer and bound proteins were detected with rabbit anti-GST antibody (Santa Cruz Biotechnology) and donkey anti-rabbit-horseradish peroxidase antibody (GE Healthcare), preceded by an additional three washes. Protein binding was visualized using Supersignal West Pico chemiluminescent reagent (Pierce) following five consecutive membrane washes.

2.2.6 Analytical ultracentrifugation.

Experiments were performed using a Beckman Optima XL-1 analytical centrifuge equipped with absorbance and interference optical detection systems (Beckman Coulter) at the Center for Analytical Ultracentrifugation of Macromolecular Assemblies at the University of Texas Health Science Center, San Antonio (UTHSCSA). Tom1 TBD (MW: 6.1 kDa), Tollip GAT (MW: 11.5 kDa), and N-terminal fluorescein-ubiquitin (MW: 8.6 kDa; BostonBiochem)

protein samples were prepared in 10 mM Tris-HCl, 175 mM NaCl, pH 7.0. Tom1 GAT and Tollip TBD were prepared at concentration of 20 μM while N-terminal fluorescein-ubiquitin was prepared at 1 μM. Protein samples were prepared as protein alone, mixture of two proteins, or a mixture of all three proteins. The partial specific volume of samples was 0.7337 cm^3/g. Absorbance values were collected at wavelengths of 230 nm and 515 nm (for samples containing fluorescein-ubiquitin) with a rotor speed of 60,000 rpm in which standard double-channel centerpieces were used at a constant temperature of 20°C. Sedimentation velocities were analyzed using the UltraScan software suite as described [[49], http: //www.ultrascan.uthscsa.edu] and calculations were performed at the Bioinformatics Core Facility at UTHSCSA. Data were first subjected to 2D spectrum analysis with simultaneous removal of time-invariant noise [50]. This was followed by enhanced van Holde-Weischet analysis [51], genetic algorithm refinement [52], and Monte Carlo analysis [53].

2.2.7 Protein-protein interaction studies through surface plasmon resonance.

Protein-protein interaction studies measuring dissociation constants were measured using a Biacore X-100. At room temperature, 0.5 mM $NiCl_2$ was saturated on the sensor chip surfaces in each cycle. A solution of 10 nM His-tagged Tom1 protein was used for immobilization on NTA sensor chip using running buffer 10 mM HEPES (pH 7.4), 150 mM NaCl, 50 μM EDTA, and 0.005% P20. Protein analytes were prepared at varying concentrations in running buffer. Protein analytes were injected over both control and experimental sensor channels. R.U.s of experimental sensor channel were measured and corrected by subtraction of the R.U.s from the control sensor channel. Dissociation constants (K_D) values were calculated with BIAevaluation software, version 2.0 (GE Healthcare).

2.2.8 Lipid-protein binding studies through SPR detection.

Liposome binding studies measured dissociation constants using a Biacore X-100. Lipid films were created by mixing 3-5% PtdIns(3)P (dissolved in chloroform/methanol/water, 65:35:8) with DOPC and drying with nitrogen gas. Lipid films were then dried overnight in a desiccator and resuspended in 0.5 mL of 20 mM HEPES, 100 mM NaCl, pH 6.8. Lipids were incubated in 67°C for 30 min, and mixed with a vortex every 10 min. Lipids were then frozen in liquid nitrogen and thawed at 67°C for a total of three cycles. Next, liposomes were sonicated 8 times in 30 sec on, 30 sec off cycles. After sonication, liposomes were extruded with 400 μm membranes. L1 sensor chip (GE Healthcare) was subjected to cleaning with 40 mM N-octyl-β-D-glucopyranoside, followed by wash steps prior to immobilizing liposomes on the chip. Approximately 4,000-6,000 R.U.s of liposomes were immobilized on the sensor chip followed by a 60-sec 100 mM NaOH wash at a flow rate of 30 μL/min. As indication of sensor chip coverage and to block uncovered surfaces, 0.1 mg/ml BSA was flowed over the surface of the sensor chip for 300 sec at a flow rate of 5 μL/min, resulting in responses less than 100 R.U.s. Protein analytes were prepared at varying concentrations in running buffer. Protein analytes were injected over both control (DOPC, no PtdIns(3)P) and PtdIns(3)P sensorchip channels. R.U.s of PtdIns(3)P sensor channel were measured and corrected by subtraction of the R.U.s from the control sensor channel. K_D values were calculated with BIAevaluation software, version 2.0 (GE Healthcare).

2.2.9 NMR titrations.

NMR experiments were performed using a Bruker 600 MHz equipped with a TBI probe and at 25°C. Binding of Tollip TBD to PtdIns(3)P was investigated using ^{15}N Tollip TBD with titrations of c4PtdIns(3)P in 20 mM d_{11}-Tris-HCl (pH 7.0), 50 mM KCl, 1 mM d_{18}-DTT, and 1

mM NaN_3. ^{15}N-TBD had a concentration of 100 μM and molar ratios between ^{15}N-TBD and PtdIns(3)P and were 1:0, 1:1, 1:2, and 1:4. ^{15}N-chemical shifts were referenced indirectly using frequency ratios as described by Wishart and colleagues [54]. Backbone and side chain resonance were previously assigned by Dr. Shuyan Xiao using a series of three-dimensional NMR experiments (data not shown). Spectra were processed with Topspin and NMRPipe [55].

Chapter 3: Results and Discussion

3.1 Subcellular localization effect due to mutations that disrupt Tom1- Tollip association.

Heteronuclear single quantum correlation (HSQC) and nuclear Overhauser effect (NOE) analyses of ^{15}N Tom1 GAT -Tollip TBD complex (performed by Dr. Shuyan Xiao in our lab) identified Tom1 GAT and Tollip TBD interacting residues (data not shown). Key-binding residues of both proteins were replaced by alanine residues using the site-directed mutagenesis method. Single and double mutant Tollip TBD and Tom1 GAT proteins were purified and their binding affinities were measured against either the wild-type or mutant binding partner using SPR detection. Binding affinities of these mutants were compared to the wild type proteins, with data shown in Table 1. With the exception of Tollip TBD F21A-Tom1 GAT N230A, the SPR data was collected and processed by Dr. Shuyan Xiao. Fold-reduction in binding ranged from 83-fold reduction to 22,000-fold reduction for these experiments. In addition, data for the binding of full length Tom1 and Tollip is also shown in Table 1. The binding of full-length proteins had a higher affinity (0.67 nM versus 0.23 nM) than the binding of wild type Tollip-TBD and Tom1-GAT domains. This is likely due to the fact that Tollip experiences dimerization while Tollip TBD remains in monomer form (the TBD construct lacks the CUE domain, which is responsible for dimerization of Tollip).

As part of this study, the binding affinity was determined between two mutant binding partners, Tom1 GAT N230A and Tollip TBD F21A. This data is also shown in Table 1. Tom1 GAT N230A and Tollip TBD F21A both exhibited the strongest reduction in binding to its wild-type binding partner. A fold reduction of 95,000 was observed in the binding between the two

mutant domains. Mutants that exhibited a reduced affinity (see table below) were chosen for their usage in immunofluorescence experiments.

Table 2: Dissociation constants of wild-type and mutant versions of Tom1 GAT and Tollip TBD measured using SPR detection. Mutant proteins were chosen after measuring chemical shift perturbations resulting from HSQC and by NOE analyses. For comparison purposes, the affinity of Tollip for Tom1 is shown at the bottom of the table. Statistical significance is shown by $\chi 2$ values, with acceptable values being less than 10.

Protein	K_D (nM)	Fit (χ^2)	Fold Reduction
Tom1 GAT-Tollip TBD	0.67 ± 0.02	0.05	1
Tom1 GAT E223A/R267A-Tollip TBD	N/A		
Tom1 GAT N230A-Tollip TBD	459.40 ± 7.55	0.05	690
Tom1 GAT L257A-Tollip TBD	221.0 ± 45.94	0.08	330
Tom1 GAT-Tollip TBD R9A/V12A	55.70 ± 0.82	0.06	83
Tom1 GAT-Tollip TBD D20A/R23A	82.10 ± 4.39	0.07	120
Tom1 GAT-Tollip TBD F21A	14,500 ± 2,192	8.26	22,000
Tom1 GAT-Tollip TBD F21A/L22A	N/A		
Tom1 GAT N230A-Tollip TBD F21A	63,500 ± 282	2.53	95,000
Tom1-Tollip	0.23 ± 0.07	0.72	

3.2 Disrupting the subcellular co-localization of Tom1 and Tollip causes mis-localization of Tollip

To investigate the effects in the localization of both Tom1 and Tollip when the association between the two proteins is disrupted, cell-based immunofluorescence experiments were performed using HeLa cells. Tollip protein contained a N-terminal EGFP tag, whereas Tom1 was fused with a 3X-FLAG tag. Early endosomal antigen 1 (EEA1) was employed as an endogenous marker for early endosomal compartments, as it functions in the fusion of early endosome to endosome vesicles [56]. Secondary antibody for Tom1 and EEA1 visualization

were conjugated to Cy 3. Wild-type FLAG-Tom1 (Cy 3) and EGFP-Tollip were individually expressed (Fig. 10). To track subcellular localization of Tollip in early endosomes, EEA1 was employed. Tollip appears to be located on punctate endosomal structures and partially co-localizes with EEA1. This partial co-localization is likely due to Tollip's function not being limited to early endosomes. This observation coincides with previously published literature showing that Tollip also partially co-localizes with Hrs, which is mainly localized to MVBs [7]. Therefore, Tollip may function in both early endosomes and MVBs. Tom1 was shown to localize diffusely distributed in the cytosol (Fig. 10). When Tom1 and Tollip were co-expressed, Tom1 co-localized with Tollip (Fig. 10). Thus, Tollip appears to effectively recruit Tom1 to endosomal structures [7].

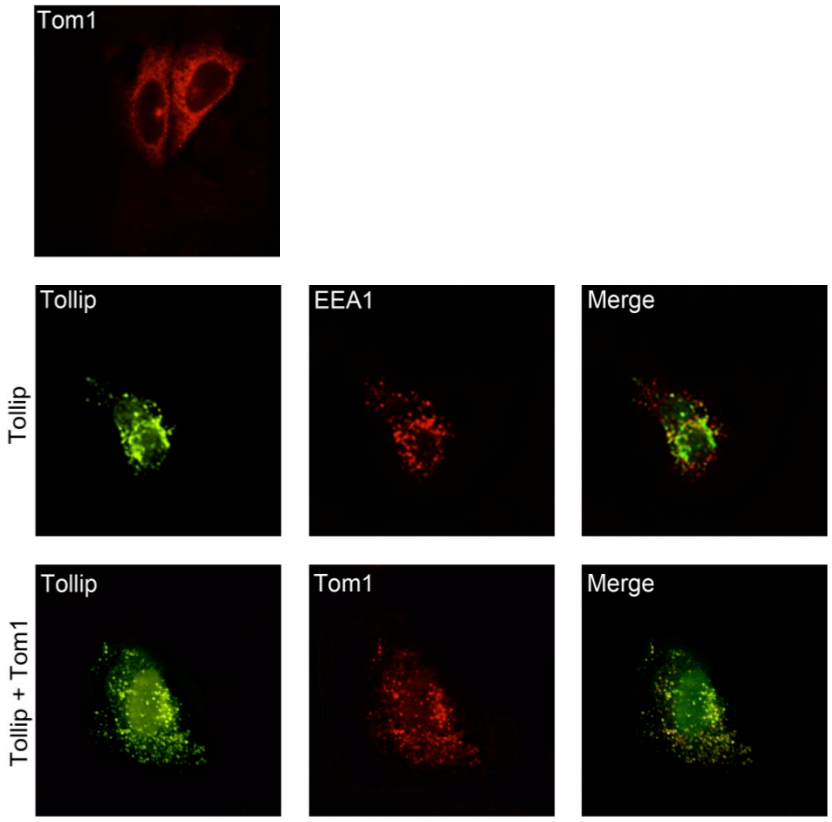

Figure 10: Tom1 and Tollip and their relative subcellular localizations in HeLa cells when overexpressed alone and together. Tom1 and EEA1 were imaged using an anti-FLAG antibody conjugated with Cy 3, while Tollip was fused with EGFP.

EGFP-Tollip mutants F21A, F21A/L22A, and D20A/R23A were co-expressed with wild-type FLAG-Tom1 (Fig. 11). The localization of the majority of Tom1 remained in the cytosol in all cases, however, some of the protein remains co-localized with Tollip. Unexpectedly, the localization of the Tollip mutants shifted as well. Tollip appears to be distributed between the cytosol and endosomal structures, with the majority of Tollip located on endosomal structures.

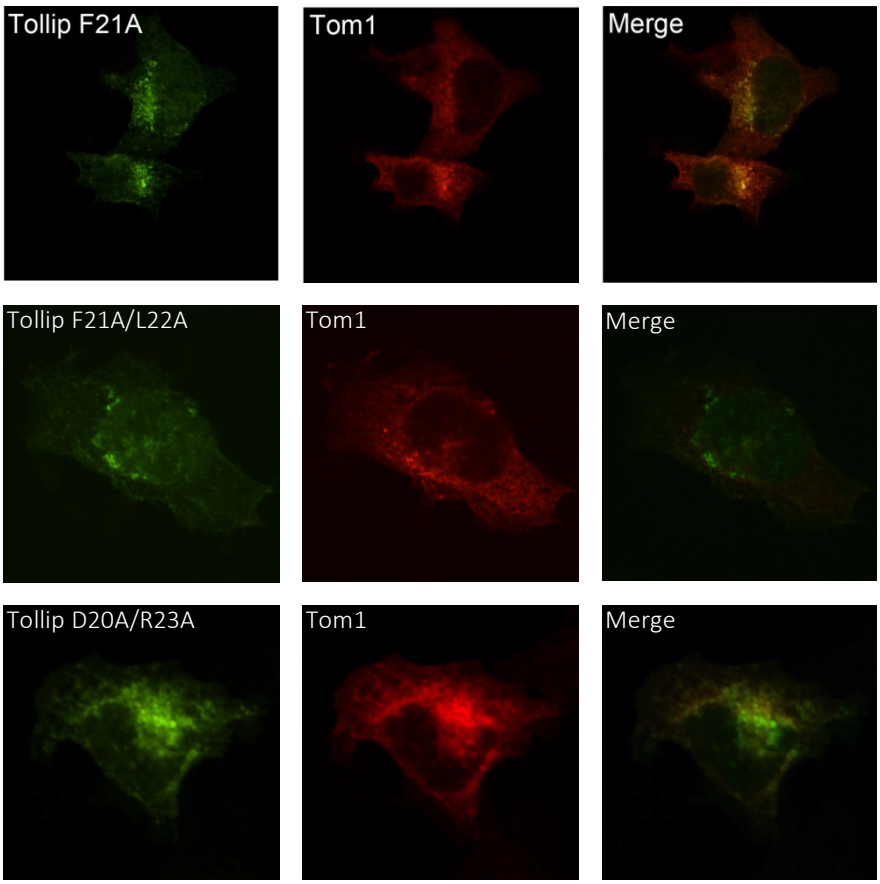

Figure 11: Subcellular localization of Tom1-defective binding mutants of Tollip with wild type Tom1. Tom1 was imaged using an anti-FLAG antibody conjugated with Cy 3, whereas Tollip was fused to EGFP.

Tollip-interacting mutants of Tom1 were also generated. Tom1 N230A, L257A, and E223A/R267A were co-expressed with wild type EGFP-Tollip to observe mis-localization resulting from disrupting the binding between Tollip and Tom1 (Fig. 12). Tom1 mutant was found distributed between both the cytosol and endosomal structures in most cases. There also

unexpectedly appears to be Tollip distributed between both the cytosol and endosomal structures, as observed in Fig. 12.

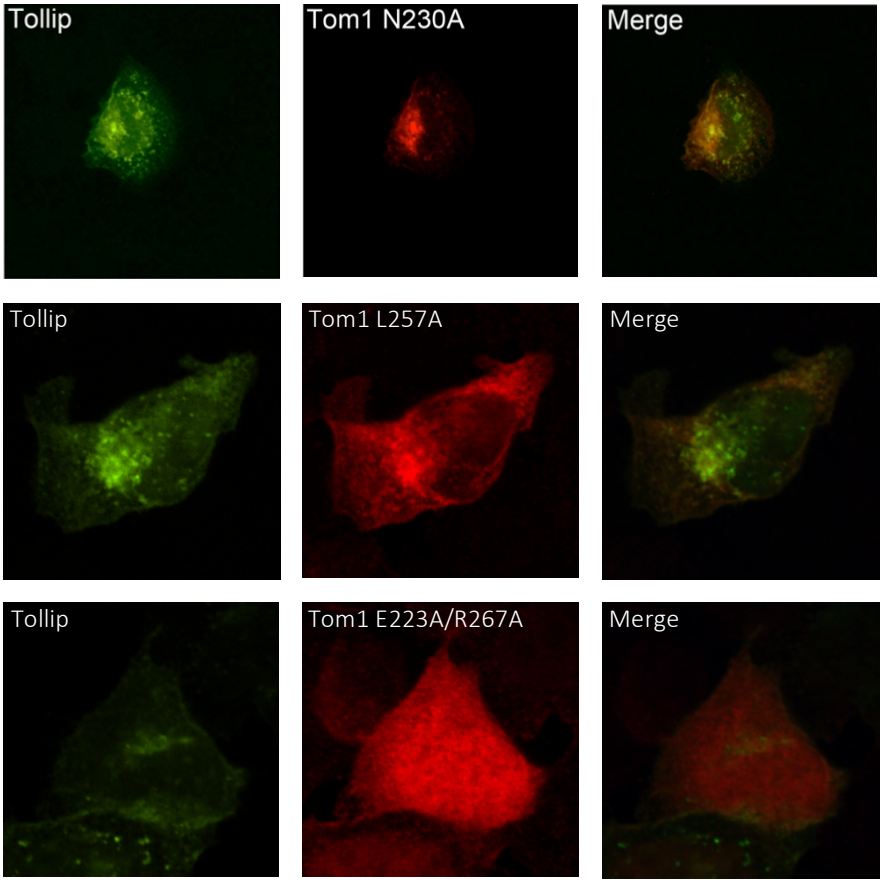

Figure 12: Subcellular localization of Tollip-defective binding mutants of Tom1 with wild-type Tollip. Tom1 was imaged using an anti-FLAG antibody conjugated with Cy 3, while Tollip was fused to EGFP.

Tom1 N230A and Tollip F21A binding mutants, which exhibit a ~90,000-fold reduction in affinity compared with the wild-type proteins (Table 1), were also co-expressed to determine whether a greater mis-localization of the two proteins would be more evident (Fig. 13). Tom1 N230A appeared to be distributed mainly in the cytoplasm of the cell. Tollip F21A was mainly distributed in the cytosol, however there was significant punctate localization of Tollip, indicating that Tollip still may be localized to the endosome. The level of mis-localization of both Tom1 N230A and Tollip F21A seems to be much higher than that seen in mutants that were

overexpressed with its wild type binding partner, supporting the hypothesis that lack of association alters the subcellular localization of the proteins.

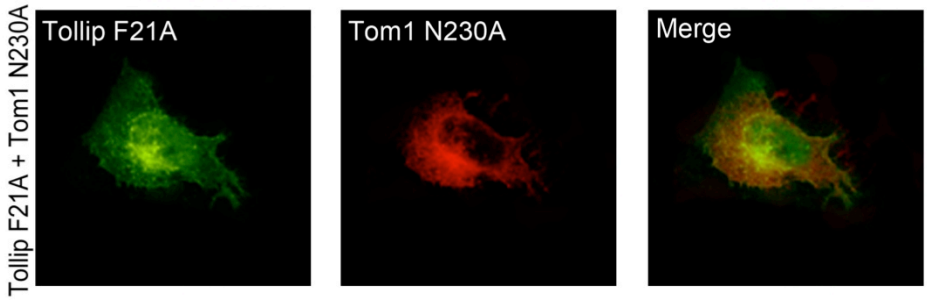

Figure 13: Tollip F21A and Tom1 N230A and their relative localizations when overexpressed together. Tom1 was imaged using an anti-FLAG antibody conjugated with Cy3, while Tollip was fused to EGFP

.

As control experiments, Tom1 and Tollip mutants were overexpressed alone to confirm that their mis-localization depends upon the corresponding binding partner (Fig. 14). All mutant localizations seem unchanged except for Tom1 E223A/R267A. Tom1 appears in the nucleus and the cytosol of the cell, with Tom1 being most concentrated in the nucleus. Tom1 E223A/R267A remains nuclear even when it is co-expressed with wild-type Tollip (Fig 14). The consequences of the nuclear localization of this mutant remain to be investigated.

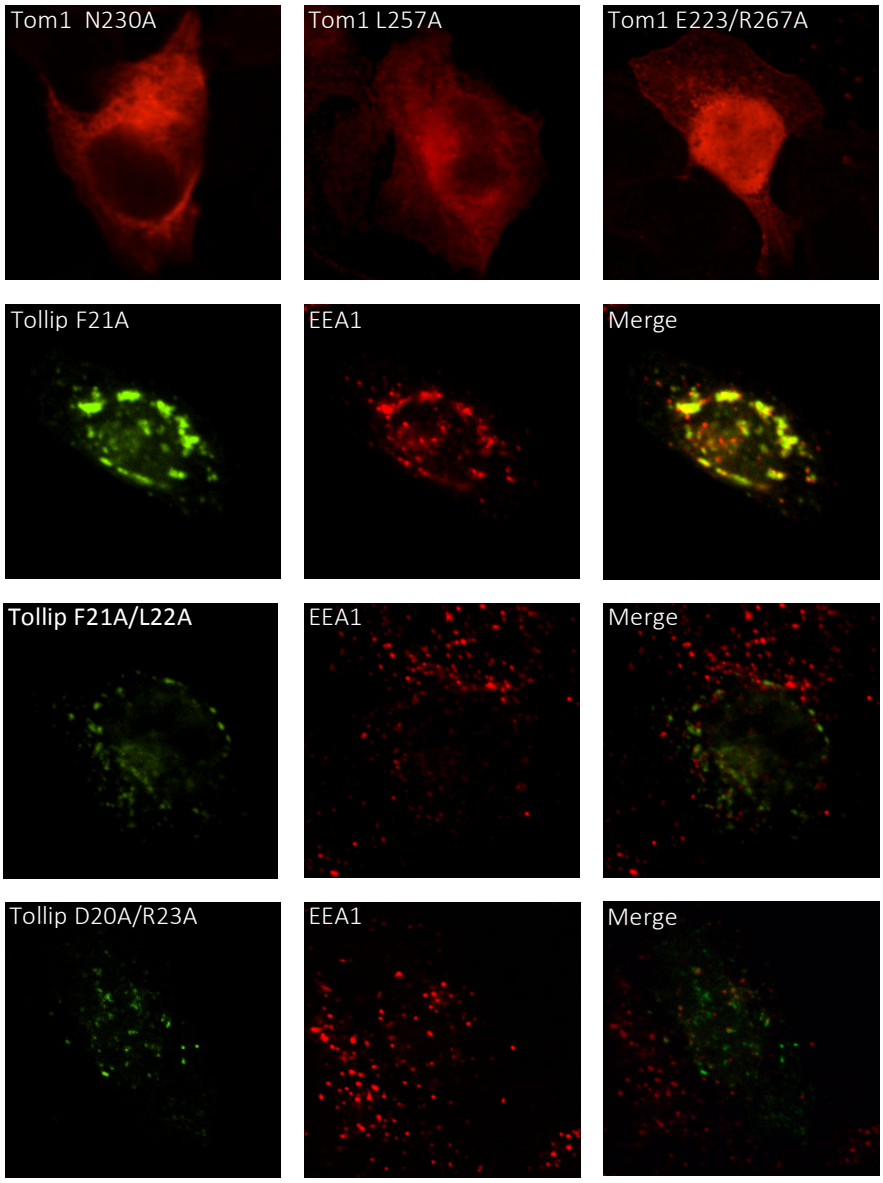

Figure 14: Subcellular localization of individual defective-binding Tom1 and Tollip mutants in HeLa cells. Tom1 and EEA1 were imaged using a secondary antibody conjugated with Cy3, while Tollip was fused to EGFP.

In summary, Tom1 experienced some mis-localization due to disrupting the binding between Tom1 GAT and Tollip TBD. However, some of the Tom1 population remained co-localized with Tollip on punctate structures. It is not surprising that some co-localization remains, as the K_D of Tom1 GAT N230A binding to Tollip TBD F21A (mutant binding partners with the highest fold reduction in binding) is still within the μM range. Therefore, the binding

between Tom1 and Tollip was incompletely disrupted. The surprising results were that the localization of Tollip was also changed when both Tollip and Tom1 were co-expressed together and the association between Tom1 and Tollip is drastically reduced via the Tom1 GAT and Tollip TBD domains. This mis-localization of Tollip in the cytosol did not occur when only Tollip is expressed. This may indicate that the presence of Tom1 may serve to direct Tollip to specific cell signaling pathways. When Tom1 is present in the cell, but not bound to Tollip, Tollip seems to be directed away from the endosomal pathway, and perhaps directed toward the innate immunity pathway. When Tom1 is present in the cell and bound to Tollip, Tollip seems to remain committed to the endosomal pathway, just as it is in the absence of Tom1. It would be interesting to determine in future studies if any of Tom1's additional ligands could prevent Tom1 binding to Tollip, recreating the effect observed when binding between Tom1 and Tollip is drastically reduced.

3.3 Tom1 inhibits the binding of Tollip to PtdIns(3)P

Lipid protein overlay assays (LPOA) were used to demonstrate the binding of Tollip to nitrocellulose membranes blotted with concentration gradients of PtdIns(3)P with and without the binding of Tom1. These experiments were performed with the help of Kristen Fread, an undergraduate researcher in the Capelluto lab. To visualize the binding of GST-Tollip, anti-GST was used as a primary antibody followed by a secondary antibody conjugated to horseradish peroxidase (HRP). For inhibition experiments, an appropriate amount of Tom1 was pre-incubated with Tollip prior to binding to the nitrocellulose membranes. Tom1 incubated with Tollip in a 0.5-fold manner was shown to significantly decrease binding of Tollip to PtdIns(3)P, while in a 1:1 fold ratio, the binding was completely abolished (Fig. 15). This indicates that Tom1 has a strong inhibitory effect on Tollip. Through additional experiments, it was shown that

GST-Tom1 does not bind to PtdIns(3)P (data not shown). As a control, Tollip F21A and Tom1 N230A proteins were generated in which the binding interface of Tollip TBD and Tom1 GAT is disrupted. These mutant proteins were used in the same method described above; Tollip F21A was preincubated with Tom1 N230A prior to binding to nitrocellulose membranes containing PtdIns(3)P. In this experiment, the inhibitory effect of Tom1 on Tollip binding to PtdIns(3)P was reversed, indicating that perhaps the interaction between Tom1 GAT and Tollip TBD is necessary for inhibition. To confirm this, it was determined that Tom1 GAT is sufficient to inhibit GST Tollip from binding to PtdIns(3)P and also that Tom1 GAT does not have a strong inhibitory effect on Tollip C2 binding to PtdIns(3)P (data not shown). Almost no change was observed in Tollip binding to PtdIns(3)P in the presence of Tom1 (Fig. 15). A potential function of this inhibition by Tom1 could be that perhaps Tollip is released from endosomal membrane as it commits for its ubiquitinated cargo transport function.

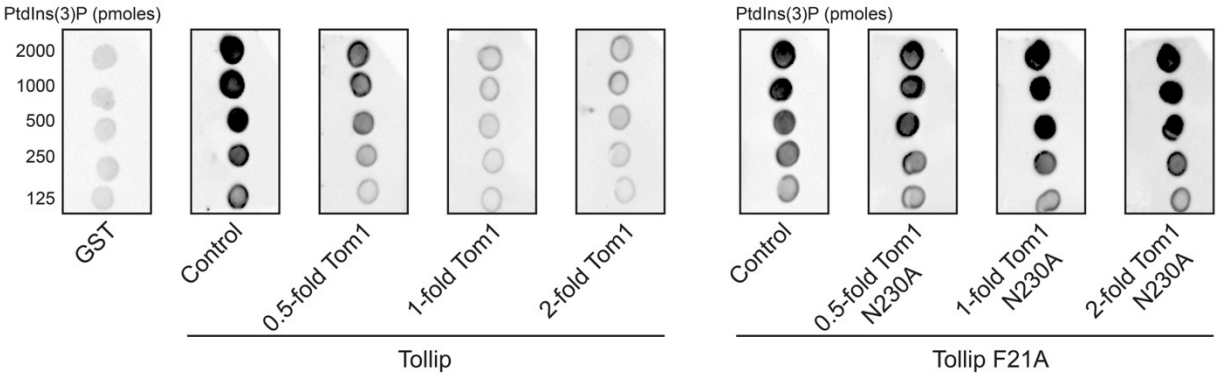

Figure 15: Effects of Tom1 on the binding of Tollip to PtdIns(3)P. Lipid-protein overlay assays in which wild type or mutant Tollip was pre-incubated with or without wild type or mutant Tom1 prior to binding to PtdIns(3)P immobilized on nitrocellulose membranes.

3.4 Tom1 GAT, but not Tollip TBD, weakly binds PtdIns(3)P.

In order to confirm that our original model of Tollip enabling the recruitment of Tom1 to endosomal membranes, it was necessary to check whether Tom1 binds PtdIns(3)P to confirm a recent study that reported binding of Tom1 GAT to PtdIns(3)P [23]. This study investigated this

using lipid protein overlay assays with a protein concentration of 15 μg/mL, which is 15-fold higher than concentrations used in the literature using this assay. Therefore, it was suspected that the reported interaction between Tom1 GAT and PtdIns(3)P may have been a non-specific binding interaction.

Initially, an ^{1}H-^{15}N heteronuclear single quantum coherence (HSQC) was performed by a graduate student in the Capelluto lab, Xiaolin Zhao, (data not shown) to detect any weak binding of Tom1 GAT to PtdIns(3)P. ^{1}H-^{15}N HSQC can be a very sensitive tool for weak protein-protein interactions in which each chemical signal represents the amide backbone of a single residue or side chains involving amide groups. Small spectral shifts can be measured as chemical shift perturbations and can give information about which residues of the labeled protein are involved in the binding. In this experiment, ^{15}N-labeled Tom1 GAT was titrated with an excess of PtdIns(3)P, and small chemical shifts were observed, indicating weak binding of Tom1 GAT to PtdIns(3)P. Upon observing this binding, a SPR experiment was designed to determine the affinity value of Tom1 GAT for PtdIns(3)P. Weak binding was observed when concentrations of Tom1 GAT (4.38-140 μM) were flowed over the L1 sensor chip surface containing PtdIns(3)P liposomes (Fig. 16). Results were analyzed using Biacore Evaluation software and an average K_D value of 18.1 ± 2.1 μM was obtained, with an average χ^2 value of 0.342 ± 0.013. The binding of GAT to PtdIns(3)P liposomes detected by SPR is relatively weak. However, this affinity may be relevant for Tom1, since it may only be able to bind to PtdIns(3)P when the levels of cellular PtdIns(3)P are increased, like during bacterial infections [24].

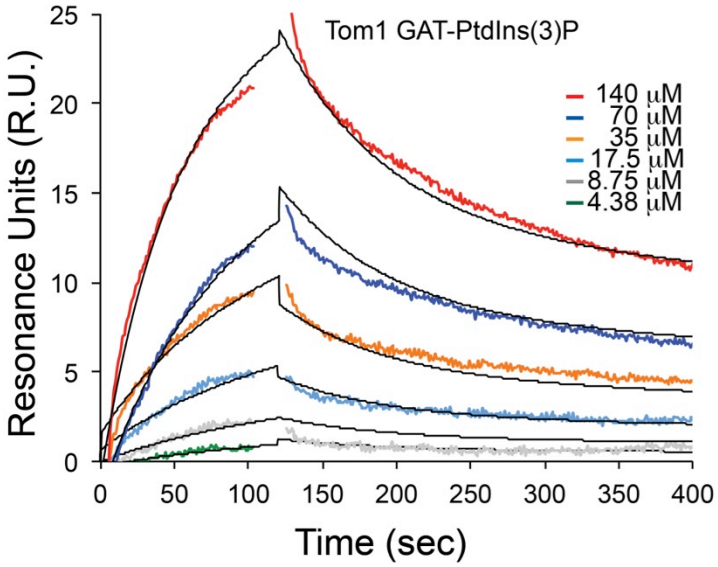

Figure 16: Tom1 GAT binding to PtdIns(3)P liposomes. Increasing concentrations of Tom1 GAT flowed across the surface of the L1 sensor chip previously immobilized with PtdIns(3)P:DOPC liposomes. Response units (R. U.) measured by SPR.

^{1}H-^{15}N HSQC was also performed in which labeled ^{15}N-Tollip TBD was titrated with increasing amounts (ranging from 1:1 to 1:4) of PtdIns(3)P (Fig. 17). No chemical perturbations were observed on any chemical signals, demonstrating that Tollip TBD does not bind to PtdIns(3)P.

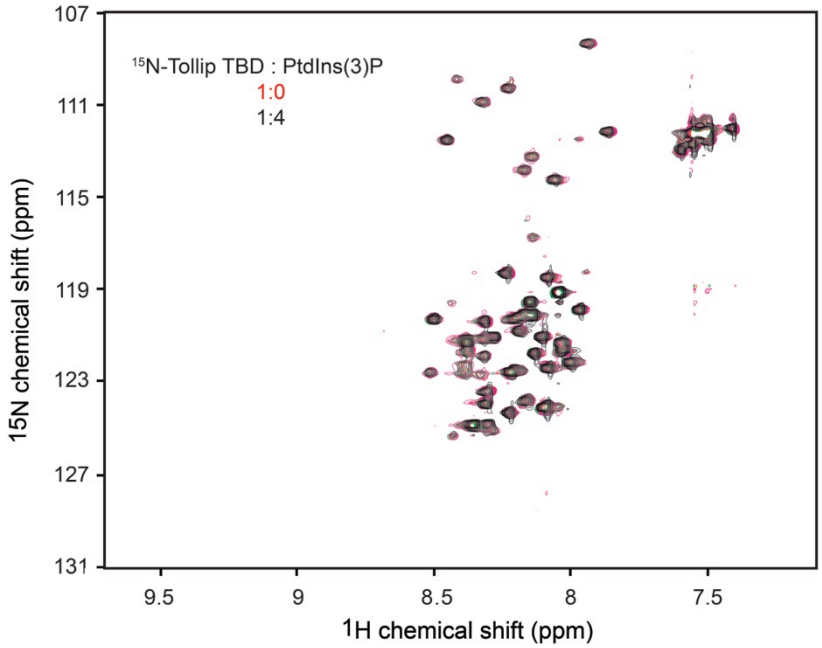

Figure 17: ^{15}N-HSQC analysis of ^{15}N-Tollip TBD titrated by PtdIns(3)P. Ranges of PtdIns(3)P tested included 1:0 to 1:4, only 1:4 PtdIns(3)P is shown for simplicity. ^{15}N-Tollip TBD without PtdIns(3)P is shown in red, whereas ^{15}N-Tollip TBD with 4-fold excess of PtdIns(3)P is shown in black.

3.5 To determine whether Tom1 GAT, Tollip TBD, and ubiquitin can form a heterotrimer.

Analytical ultracentrifugation (AUC) was employed to measure the sedimentation velocity in order to determine whether the Tom1 GAT domain can simultaneously bind Tollip TBD and ubiquitin. AUC is a useful technique for investigating protein-protein interactions. During ultracentrifugation, solutes experience forces from sedimentation, diffusion/buoyancy, and friction [57]. Sedimentation or gravitational forces exist as a result of the centrifugal force field. For ultracentrifugation, the rotor is usually spun at or near 60,000 rpm. For example, a solute that has a mass of 1 gram would experience a force of 250 kg when spun at this speed in a typical AUC rotor [58]. The equation $M_p\omega^2 r$ represents the gravitational force experienced by a particle in a sedimentation experiment, where M_p is the mass of the macromolecule, ω is the angular velocity in radians/second, and r is the distance from the center of rotation [57]. However, the gravitational force is opposed by the presence of a solvent such as sucrose. The mass of the solvent and the amount of solvent displaced needs to be accounted for to obtain the true force on the macromolecule. Therefore, the equation $M_b=M_p(1-\bar{v}\rho)$ represents the buoyant mass of the particle, with $\bar{v}$ being the partial specific volume of the particle and ρ being the density of the solvent [57]. The frictional force is calculated by fv, in which f is the frictional coefficient and v is the velocity of the particle [57]. These forces upon a macromolecule subjected to velocity experiments balance each other after a short period of time. The sedimentation coefficient s, is obtained from the Svedberg equation, $s = \frac{v}{\omega^2 r} = \frac{M_b}{f}$ [57]. Therefore, by determining the sedimentation coefficient, the frictional coefficient, f, can also be determined, which is necessary for calculating the diffusion coefficient, by the equation $D = \frac{RT}{N_a f}$, in which R is the gas constant, T is the absolute temperature, and N_a is Avogadro's number [57]. The friction coefficient offers insight into the shape of a macromolecule. The frictional ratio, f/f_o,

is a comparison of the experimental frictional coefficient to a theoretical frictional coefficient, in which the macromolecule of the same molecular weight would be a perfect sphere [59]. Therefore, a globular macromolecule should have a frictional ratio near 1. AUC instruments typically monitor the relative radius (r) and concentration (c) of the macromolecule, ω, and time (t) simultaneously. The Lamm equation, $\partial C\frac{\partial c}{\partial \mathrm{t}} = D\left[\frac{\partial^2 c}{\partial r^2} + \frac{1}{r}\frac{\partial c}{\partial r}\right] - s\omega^2\left[r\frac{\partial c}{\partial r} + 2c\right]$, then allows the AUC software to compute the sedimentation coefficient, s, and the diffusion coefficient, D [50]. The Lamm equation can be altered to $C_T = \sum_{i=1}^{n} c_i L(s_i.D_i)$ for an experiment with a mixture of solutes, rather than a single solute [50]. In this version of the Lamm equation, C_T is the total concentration of all solutes in the experiment while c_i, s_i, and D_i represent the partial concentration, sedimentation coefficient, and diffusion coefficient of each solute present [50]. L represents the original Lamm equation presented above [50].

In this experiment in which the trimeric nature of a complex formed by Tom1 GAT, Tollip TBD, and ubiquitin was investigated, proteins were monitored at an absorbance of 230 nm for samples containing Tom1 GAT alone, Tom1 GAT-Tollip TBD, and Tollip TBD alone. A wavelength of 230 nm was chosen as it is in the wavelength range at which peptide bonds commonly absorb and was a better choice than 280 nm, as Tom1 GAT does not contain any tyrosine or tryptophan residues. The ubiquitin used in these experiments was fluorescein conjugated; all samples containing ubiquitin (ubiquitin alone, Tom1 GAT-ubiquitin, Tollip TBD-ubiquitin, and Tom1 GAT-Tollip TBD-ubiquitin) were monitored at a wavelength of 515 nm, where fluorescein emits light energy.

Data for all AUC experiments is shown in Figure 18. Panels a-e illustrates a plot of each protein or protein complex as a function of its frictional ratio, partial concentration, and molecular weight (experimental). Panels a-c monitored protein at a wavelength of 230 nm, while

panels d-e monitored ubiquitin protein at 515 nm. Panel f displays a table of calculated values of molecular weights, sedimentation coefficients, and frictional ratios of each sample in the experiment. The sample containing Tollip TBD alone resulted in a calculated molecular weight of 6.993 kDa (actual 6.129 kDa), sedimentation coefficient of 0.744 s^{-13}, and a frictional ratio of 1.785. Tollip TBD is an intrinsically disordered protein, which accounts for Tollip TBD having the highest frictional ratio out of the samples tested. Tollip TBD is also of the lowest molecular weight of the proteins tested, which explains it having the lowest sedimentation coefficient. The experimentally calculated molecular weight (6.993 kDa) is higher than its actual molecular weight (6.129 kDa), but this is most likely influenced by the disordered configuration/high frictional ratio. Tom1 GAT alone resulted in a calculated molecular weight of 11.243 kDa, a sedimentation coefficient of 1.462 s^{-13}, and a frictional ratio of 1.219. GAT is an alpha helical protein, giving it a narrow configuration, which explains why GAT has the lowest frictional ratio out of each protein sample tested alone. The molecular weight of GAT is the largest out of the three proteins, resulting in a high sedimentation coefficient, second only to the Tollip TBD-Tom1 GAT complex. Its calculated molecular weight of 11.243 kDa is relatively accurate when compared to its actual molecular weight of 11.497 kDa. The sample containing both Tollip TBD and Tom1 GAT resulted in a calculated molecular weight of 16.4 kDa, a sedimentation coefficient of 1.669 s^{-13}, and a frictional ratio of 1.384. These results are as expected based on current knowledge of the interaction between Tollip TBD and Tom1 GAT. Through data obtained in the Capelluto lab (not shown), it is known that the N-terminal portion of Tollip TBD folds upon binding of Tom1 GAT. This binding and folding mechanism that Tollip TBD undergoes causes a shift from a disordered conformation to a partly globular structure, resulting in a decrease in the calculated frictional ratio, upon binding of Tollip TBD to Tom1 GAT. The

ubiquitin sample alone resulted in a calculated molecular weight of 11.639 kDa, a sedimentation coefficient of 1.364 s^{-13}, and a frictional ratio of 1.253. The moderate sedimentation coefficient and frictional ratio value seem as expected for a globular-shaped protein like ubiquitin, although the calculated molecular weight is higher than expected for ubiquitin by about 3 kDa. However, this difference is typically observed when the sedimentation coefficient of ubiquitin is estimated. It is possible that the presence of fluorescein influences the sedimentation. In the sample containing all three proteins (Tollip TBD, Tom1 GAT, and ubiquitin), the molecular weight calculated was 9.531 kDa while the sedimentation coefficient and frictional ratio was 1.320 s^{-13} and 1.196, respectively. These values were obtained by monitoring the ubiquitin protein at 515 nm. It was suspected that the binding of Tollip TBD to Tom1 GAT would prevent the binding of ubiquitin to either Tom1 GAT ubiquitin binding site 1, Tom1 GAT ubiquitin binding site 2, or potentially inhibit ubiquitin binding to both sites on Tom1 GAT. These results suggest that ubiquitin does not bind to Tom1 GAT when Tollip TBD is bound. The calculated molecular weight, sedimentation coefficient, and frictional ratio are similar in values to those found for ubiquitin alone. This suggests that is very likely that a complex formed does not involve ubiquitin. It is worth noting that the calculated molecular weight of ubiquitin and the ubiquitin-Tom1 GAT-Tollip TBD differ by slightly over 2 kDa, however this is may be due to experimental variation and is not a large enough value to be attributed the binding of the Tom1 GAT-Tollip TBD complex, even if accompanied by conformational changes.

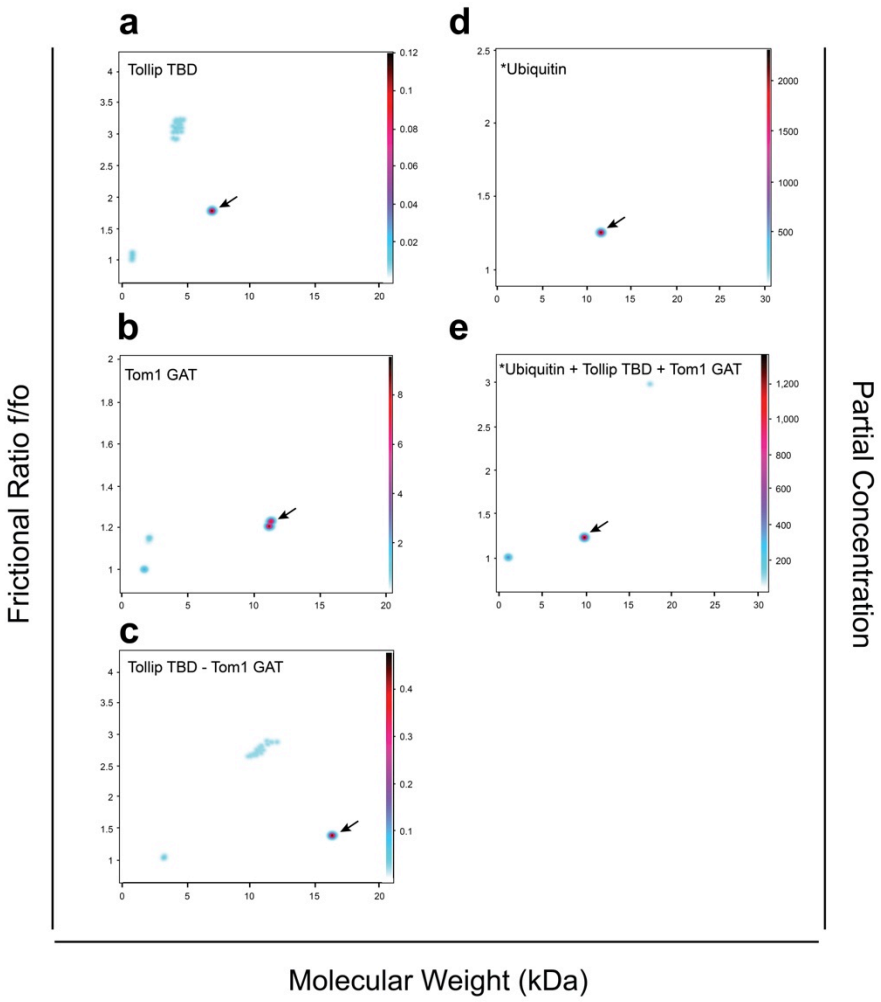

f

	Molecular Weight (kDa)	Sed. Coefficient (s^{-13})	Frictional Ratio (f/fo)
Tollip TBD	6.993 (6.941, 7.046) [6.129]	0.744 (0.739, 0.749)	1.785 (1.772, 1.798)
Tom1 GAT	11.243 (11.073, 11.413) [11.497]	1.462 (1.439, 1.484)	1.219 (1.198, 1.241)
Tollip TBD-Tom1 GAT	16.400 (16.276, 16.523) [17.626]	1.669 (1.669, 1.669)	1.384 (1.377, 1.391)
* Ubiquitin	11.639 [8.567]	1.384	1.253
* Ubiquitin-Tollip TBD-Tom1 GAT	9.531 (9.399, 9.662) [26.193][1]	1.320 (1.316, 1.324)	1.196 (1.187, 1.205)

Figure 18: Sedimentation velocity experiments in which the binding of ubiquitin-fluorescein to the Tollip TBD-Tom1 GAT complex was analyzed. (a-c) Tollip TBD, Tom1 GAT, and Tollip TBD-Tom1 GAT protein monitered at 230 nm. (d-e) Ubiquitin-fluorescein and ubiquitin-fluorescein + Tollip TBD + Tom1 GAT analyzed at 515 nm. (f) Experimental molecular weights, sedimentation coefficients, and frictional ratios listed for each sample analyzed.

Chapter 4: Summary and Conclusions

The purpose of this thesis project was to further characterize the function of the binding of Tom1 and Tollip with each other. Substantial structural data had already been gathered by previous members of our lab (data not shown), however additional functional data was necessary to complement the study. To gather information about the function of this association, a variety of techniques were used, including cellular-based immunofluorescence assays, LPOA, SPR, NMR, and AUC.

In this thesis study, it was determined that the binding of Tom1 with Tollip may serve to direct Tollip to its cellular commitments. This was observed using cell-based experiments; Tollip (in addition to Tom1) was mis-localized upon the disruption of the Tollip TBD and Tom1 GAT binding interface. Interestingly, it was additionally seen that the binding of Tom1 actually inhibits the ability of Tollip to bind to PtdIns(3)P. To further develop a theory about the function of Tom1 and Tollip binding, it was also confirmed that Tom1 GAT has the ability to weakly bind to PtdIns(3)P membranes. The last objective investigated determined that when Tollip TBD binds to Tom1 GAT, ubiquitin is inhibited from binding to Tom1 GAT.

Clearly more studies are necessary to completely understand the function of the association of Tollip and Tom1 with each other, however, many inferences can be made from data obtained in this study. A likely function of Tom1 is that it serves to direct Tollip to the specific cellular pathway it will be committed to as well as to remove Tollip from the PtdIns(3)P located on the endosomal membranes. It could be possible that Tollip must be released from endosomal membranes in order to deliver ubiquitinated cargo to the lysosomal pathways. To address this hypothesis, additional experiments will be necessary to better understand the role of the adaptor proteins Tollip and Tom1 in cargo trafficking. With these and additional results, the

scientific community may be one step closer to identifying additional therapeutic targets for combating diseases associated with deficient cell cargo trafficking.

Chapter 5: Additional Work

5.1 Binding of PKCa and PKCb II C2 domains to phosphatidylserine is weakly inhibited by ubiquitin

Dr. Sharmistha Mitra had previously determined that ubiquitin inhibits the binding of Tollip C2 to PtdIns(3)P through the use of LPOA experiments. As controls of this finding, I performed additional LPOAs in which phosphatidylserine (PtdSer) was immobilized on nitrocellulose membranes and incubated with PKCα and PKCβ II C2 domains with or without the presence of 3-fold ubiquitin. As a positive control for this experiment, Vam7p PX domain with or without 4-fold ubiquitin was incubated with nitrocellulose membranes containing immobilized PtdIns(3)P. These experiments determined that ubiquitin weakly inhibited PKCα and PKCβ II C2 domains binding to PtdSer. These experiments are shown in Figure 2, panel B of the attached article.

The citation of the article is as follows:

Mitra S, Traughber CA, Brannon MK, Gomez S, and Capelluto DGS. Ubiquitin Interacts with the Tollip C2 and CUE Domains and Inhibits Binding of Tollip to Phosphoinositides. *The Journal of Biological Chemistry*. 2013;288(36):25780-25791. doi:10.1074/jbc.M113.484170.

5.2 The binding of heme to translationally controlled tumor protein (TCTP) enables dimerization of TCTP.

Determined by the laboratory of Dr. Carla Finkielstein, TCTP can dynamically switch between a conformation that allows dimerization and a conformation that does not allow dimerization. This conformational change is controlled by the binding of a TCTP ligand, hemin. To supplement this study, I determined structural similarities between F129W TCTP (used in tryptophan fluorescence) and wild type TCTP, determined dissociation constants of TCTP binding to two of its ligands using intrinsic tryptophan fluorescence, and performed a bis-sulfosuccinimidyl suberate (BS^3) cross-linking reaction to demonstrate dimerization of TCTP as a result of ligand binding.

As tryptophan (or tyrosine) residues are necessary for fluorescence spectra of proteins and TCTP lacks tryptophans, this residue was added to TCTP by replacing a phenylalanine at the position 129. To ensure that this change did not affect the structure of the protein, far-UV analysis was performed, comparing F129W TCTP to wild type TCTP (Figure S3B). No significant structural changes appeared in the spectra of F129W TCTP. To determine the dissociation constant (K_D) of TCTP to hemin, TCTP was titrated by increasing concentrations of hemin and each of the spectra was collected. The spectrum of each hemin concentration without any TCTP was collected and was used for background subtraction. With the addition of hemin, TCTP experienced significant quenching of fluorescence, indicative of conformational changes that inhibit the fluorescence of the single tryptophan (Fig. 2D). To calculate the K_D value, a non-liner regression was performed using Kaleidoscope, plotting F_{max}-F versus the concentration of hemin. The K_D value determined for the binding of hemin to TCTP was 4.83 μM (χ^2 0.000651). The same was performed for titrations of TCTP by $CaCl_2$, an additional ligand of TCTP.Fluorescence quenching was also present in this experiment, but to a much lesser extent

(Fig. 2E). The K_D value obtained for the binding of TCTP to $CaCl_2$ was 8.02±1.16 mM (χ^2 0.000348).

To complement data demonstrating that TCTP dimerization is induced by the binding of hemin to TCTP, a BS^3 cross-linking experiment was performed. TCTP was incubated with an excess of either hemin or $CaCl_2$ and BS^3. The BS^3 cross-linking reaction was quenched by the addition of Tris buffer, and samples were then analyzed on a SDS-PAGE electrophoresis gel. It was observed that a TCTP dimer was present, in addition to monomer, when TCTP was incubated with an excess of hemin and BS^3. However, only monomer species of TCTP were observed for the incubation of TCTP with an excess of $CaCl_2$ and BS^3 (Fig. S2)

The citation of the paper is as follows:

Lucas AT, Fu X, Liu J, Brannon MK, Yang J, Capelluto, D. G. S., and Finkielstein, C. V. (2014) Ligand Binding Reveals a Role for Heme in Translationally-Controlled Tumor Protein Dimerization. PLoS ONE 9(11): e112823. doi:10.1371/journal.pone.0112823.

References

1. Alberts, B., Johnson, A., Lewis J., et al. , *Molecular Biology of the Cell*. 4th Edition ed. Figure 13-49. The endocytic pathway from the plasma membrane 2002, New York: Garland Science.
2. Alberts, B., Johnson, A., Lewis, J., et al. , *Molecular Biology of the Cell*. 4th Edition ed. Figure 13-42: Three pathways to degradation in lysosomes. 2002, New York: Garland Science.
3. Husnjak, K. and I. Dikic, *Ubiquitin-binding proteins: decoders of ubiquitin-mediated cellular functions.* Annu Rev Biochem, 2012. **81**: p. 291-322.
4. Akutsu, M., et al., *Structural basis for recognition of ubiquitinated cargo by Tom1-GAT domain.* FEBS Lett, 2005. **579**(24): p. 5385-91.
5. Wang, T., et al., *The emerging role of VHS domain-containing Tom1, Tom1L1 and Tom1L2 in membrane trafficking.* Traffic, 2010. **11**(9): p. 1119-28.
6. Capelluto, D.G., *Tollip: a multitasking protein in innate immunity and protein trafficking.* Microbes Infect, 2012. **14**(2): p. 140-7.
7. Katoh, Y., et al., *Tollip and Tom1 form a complex and recruit ubiquitin-conjugated proteins onto early endosomes.* J Biol Chem, 2004. **279**(23): p. 24435-43.
8. Shields, S.B. and R.C. Piper, *How ubiquitin functions with ESCRTs.* Traffic, 2011. **12**(10): p. 1306-17.
9. Huotari, J. and A. Helenius, *Endosome maturation.* EMBO J, 2011. **30**(17): p. 3481-500.
10. Mukherjee, S.e.a., *Endocytosis.* Physiological Reviews, 1997. **77**(3).
11. Zimmermann, R., et al., *Protein translocation across the ER membrane.* Biochim Biophys Acta, 2011. **1808**(3): p. 912-24.

12. Ikeda, F., N. Crosetto, and I. Dikic, *What determines the specificity and outcomes of ubiquitin signaling?* Cell, 2010. **143**(5): p. 677-81.

13. Sadowski, M., et al., *Protein monoubiquitination and polyubiquitination generate structural diversity to control distinct biological processes.* IUBMB Life, 2012. **64**(2): p. 136-42.

14. Kirkin, V. and I. Dikic, *Role of ubiquitin- and Ubl-binding proteins in cell signaling.* Curr Opin Cell Biol, 2007. **19**(2): p. 199-205.

15. Haglund, K. and I. Dikic, *The role of ubiquitylation in receptor endocytosis and endosomal sorting.* J Cell Sci, 2012. **125**(Pt 2): p. 265-75.

16. Ciarrochi, A., D'Angelo, R., *Tollip is a Mediator of Protein Sumoylation.* PLoS One, 2009.

17. Shiba, Y., et al., *GAT (GGA and Tom1) domain responsible for ubiquitin binding and ubiquitination.* J Biol Chem, 2004. **279**(8): p. 7105-11.

18. Ren, X. and J.H. Hurley, *VHS domains of ESCRT-0 cooperate in high-avidity binding to polyubiquitinated cargo.* EMBO J, 2010. **29**(6): p. 1045-54.

19. Yamakami, M., T. Yoshimori, and H. Yokosawa, *Tom1, a VHS domain-containing protein, interacts with tollip, ubiquitin, and clathrin.* J Biol Chem, 2003. **278**(52): p. 52865-72.

20. Seet, L.F., et al., *Endofin recruits TOM1 to endosomes.* J Biol Chem, 2004. **279**(6): p. 4670-9.

21. Katoh, Y., et al., *Recruitment of clathrin onto endosomes by the Tom1-Tollip complex.* Biochem Biophys Res Commun, 2006. **341**(1): p. 143-9.

22. Seet, L.F. and W. Hong, *Endofin recruits clathrin to early endosomes via TOM1.* J Cell Sci, 2005. **118**(Pt 3): p. 575-87.

23. Boal, F., et al. , *Tom1 is a PI5P effector involved in the regulation of endosomal maturation.* Journal of Cell Science, 2015.

24. Ireton, K., et al. , *A Role for Phosphoinositide 3-Kinase in Bacterial Invasion.* Science, 1996. **274**(5288): p. 780-782.

25. Ankem, G., et al., *The C2 domain of Tollip, a Toll-like receptor signalling regulator, exhibits broad preference for phosphoinositides.* Biochem J, 2011. **435**(3): p. 597-608.

26. Li, T., J. Hu, and L. Li, *Characterization of Tollip protein upon Lipopolysaccharide challenge.* Mol Immunol, 2004. **41**(1): p. 85-92.

27. Cho, W., *Membrane targeting by C1 and C2 domains.* J Biol Chem, 2001. **276**(35): p. 32407-10.

28. Mitra, S., et al., *Ubiquitin interacts with the Tollip C2 and CUE domains and inhibits binding of Tollip to phosphoinositides.* J Biol Chem, 2013. **288**(36): p. 25780-91.

29. Azurmendi, H.F., et al., *Backbone (1)H, (15)N, and (13)C resonance assignments and secondary structure of the Tollip CUE domain.* Mol Cells, 2010. **30**(6): p. 581-5.

30. Lo, Y.L., et al., *Diversification of TOLLIP isoforms in mouse and man.* Mamm Genome, 2009. **20**(5): p. 305-14.

31. Shih, S., Prag, G., Francis, S., *<A ubiquitin binding motif required for intramolecular monounbiquitylation, the CUE domain>*. EMBO J, 2003.

32. Kang, R., Daniels, C., *<Solution Structure of a CUE-Ubiquitin Complex Reveals a Conserved Mode of Ubiquitin Binding>*. Cell, 2003.

33. Prag, G., Misra, S., Jones, E., *<Mechanism of Ubiquitin Recognition by the CUE Domain of Vps9p>*. Cell, 2003.

34. Brissoni, B., et al., *Intracellular trafficking of interleukin-1 receptor I requires Tollip.* Curr Biol, 2006. **16**(22): p. 2265-70.

35. Iwasaki, A. and R. Medzhitov, *Regulation of adaptive immunity by the innate immune system.* Science, 2010. **327**(5963): p. 291-5.

36. Jeong, E. and J.Y. Lee, *Intrinsic and extrinsic regulation of innate immune receptors.* Yonsei Med J, 2011. **52**(3): p. 379-92.

37. Doyle, S.L. and L.A. O'Neill, *Toll-like receptors: from the discovery of NFkappaB to new insights into transcriptional regulations in innate immunity.* Biochem Pharmacol, 2006. **72**(9): p. 1102-13.

38. Mayers, J.R. and A. Audhya, *Vesicle formation within endosomes: An ESCRT marks the spot.* Commun Integr Biol, 2012. **5**(1): p. 50-6.

39. Ren, X., et al., *Hybrid structural model of the complete human ESCRT-0 complex.* Structure, 2009. **17**(3): p. 406-16.

40. Jovic, M., et al., *The early endosome: a busy sorting station for proteins at the crossroads.* Histology and histopathology, 2010. **25**(1): p. 99-112.

41. Cook, D.N., D.S. Pisetsky, and D.A. Schwartz, *Toll-like receptors in the pathogenesis of human disease.* Nat Immunol, 2004. **5**(10): p. 975-9.

42. Frantz, S., J. Bauersachs, and R.A. Kelly, *Innate immunity and the heart.* Curr Pharm Des, 2005. **11**(10): p. 1279-90.

43. Frantz, S., G. Ertl, and J. Bauersachs, *Mechanisms of disease: Toll-like receptors in cardiovascular disease.* Nat Clin Pract Cardiovasc Med, 2007. **4**(8): p. 444-54.

44. Hu, Y., et al., *Tollip attenuated the hypertrophic response of cardiomyocytes induced by IL-1beta.* Front Biosci, 2009. **14**: p. 2747-56.

45. Kanzler, H., et al., *Therapeutic targeting of innate immunity with Toll-like receptor agonists and antagonists.* Nat Med, 2007. **13**(5): p. 552-9.

46. Ulevitch, R.J., *Therapeutics targeting the innate immune system.* Nat Rev Immunol, 2004. **4**(7): p. 512-20.

47. Liu, Y., et al., *Toll-interacting protein (Tollip) negatively regulates pressure overload-induced ventricular hypertrophy in mice.* Cardiovasc Res, 2014. **101**(1): p. 87-96.

48. Simonion, M.H., *Spectrophotometric and colorimetric determination of protein concentration.* Curr Protoc Mol Biol, 2006.

49. Cao, W. and B. Demeler, *Modeling analytical ultracentrifugation experiments with an adaptive space-time finite element solution of the Lamm equation.* Biophys J, 2005. **89**(3): p. 1589-602.

50. Brookes, E., W. Cao, and B. Demeler, *A two-dimensional spectrum analysis for sedimentation velocity experiments of mixtures with heterogeneity in molecular weight and shape.* Eur Biophys J, 2010. **39**(3): p. 405-14.

51. Demeler, B. and K.E. van Holde, *Sedimentation velocity analysis of highly heterogeneous systems.* Anal Biochem, 2004. **335**(2): p. 279-88.

52. Lee, D.S., et al., *Structural basis of hereditary coproporphyria.* Proc Natl Acad Sci U S A, 2005. **102**(40): p. 14232-7.

53. Mao, X., et al., *Structural bases of unphosphorylated STAT1 association and receptor binding.* Mol Cell, 2005. **17**(6): p. 761-71.

54. Wishart, D.S., et al., *1H, 13C and 15N chemical shift referencing in biomolecular NMR.* J Biomol NMR, 1995. **6**(2): p. 135-40.

55. Delaglio, F., et al., *NMRpipe - a multidimensional spectral processing system based on Unix pipes.* J Biomol NMR, 1995. **6**(3): p. 277-293.

56. Ramanathan, H., *Monoubiquitination of EEA1 regulates endosome fusion and trafficking.* Cell and Bioscience, 2013.

57. Cole, J.L., et al., *Analytical Ultracentrifugation: Sedimentation Velocity and Sedimentation Equilibrium.* 2008. **84**: p. 143-179.

58. Ralston, G., *Introduction to Analytical Ultracentrifugation.* Beckman Coulter.

59. Laue, T.M., *Advances in Sedimentation Velocity Analysis.* Biophys J, 1997. **72**.